工業技術研究院
Industrial Technology Research Institute

Remote Sensing Technology Applied to Monitor Land Subsidence in CRAF

時頻分析與地球科學研討會

主講者： 洪偉嘉 博士

October 27, 2011

Contents

1. Introduction

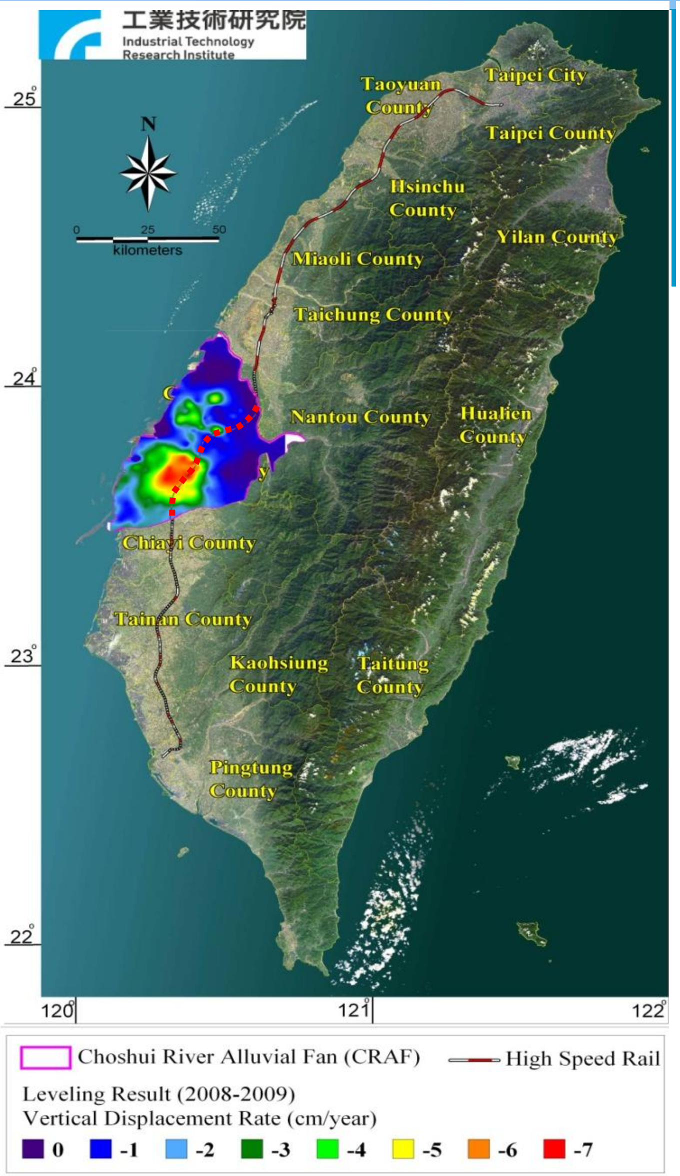

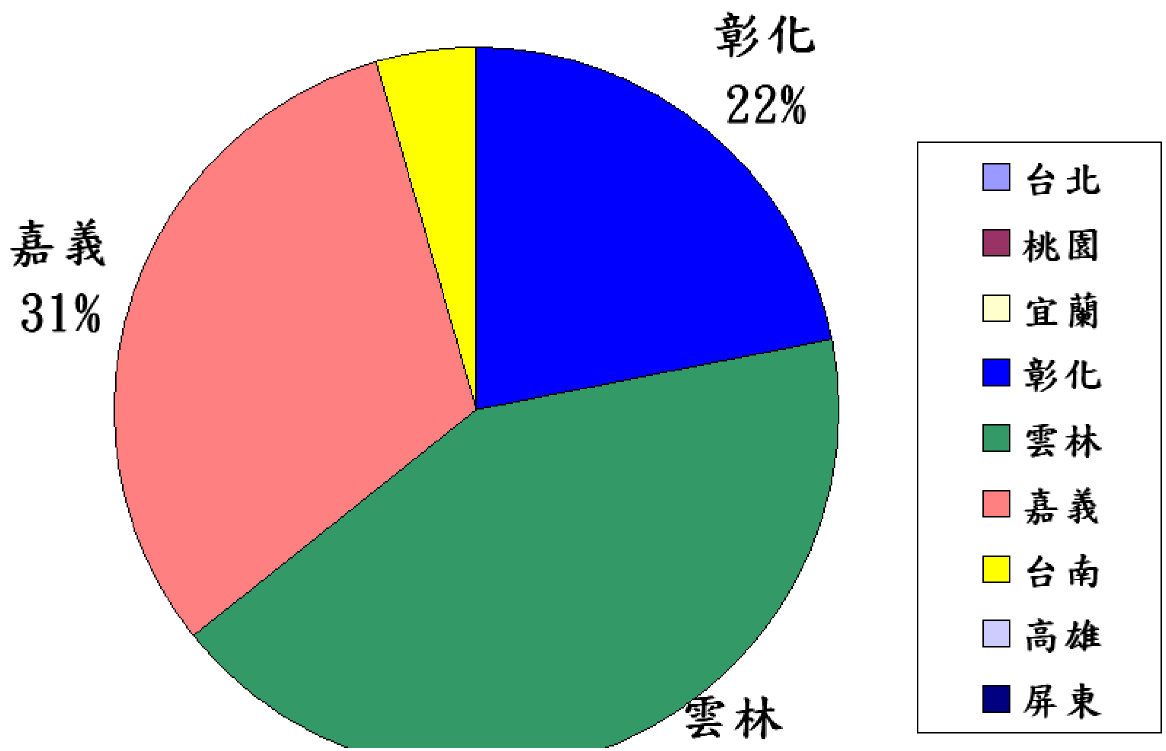

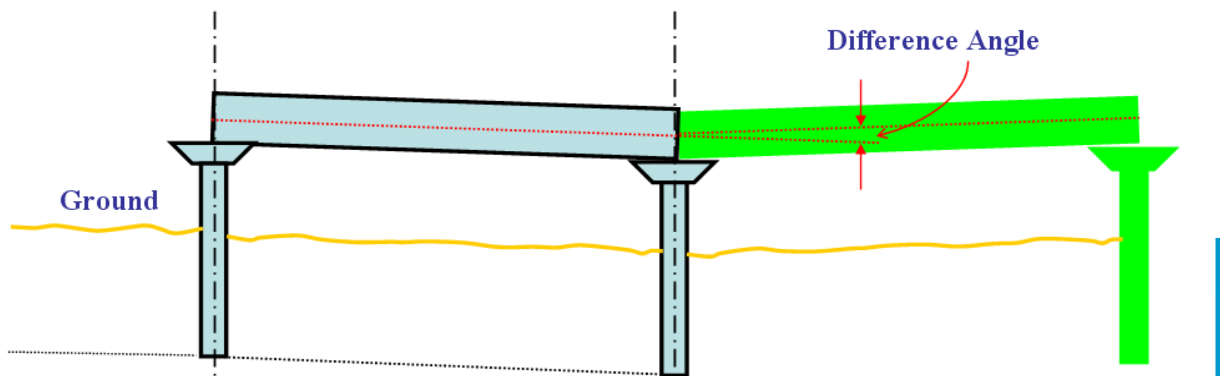

Cumulative subsidence in Changhwa County from 1992 to 2010

1992-2010

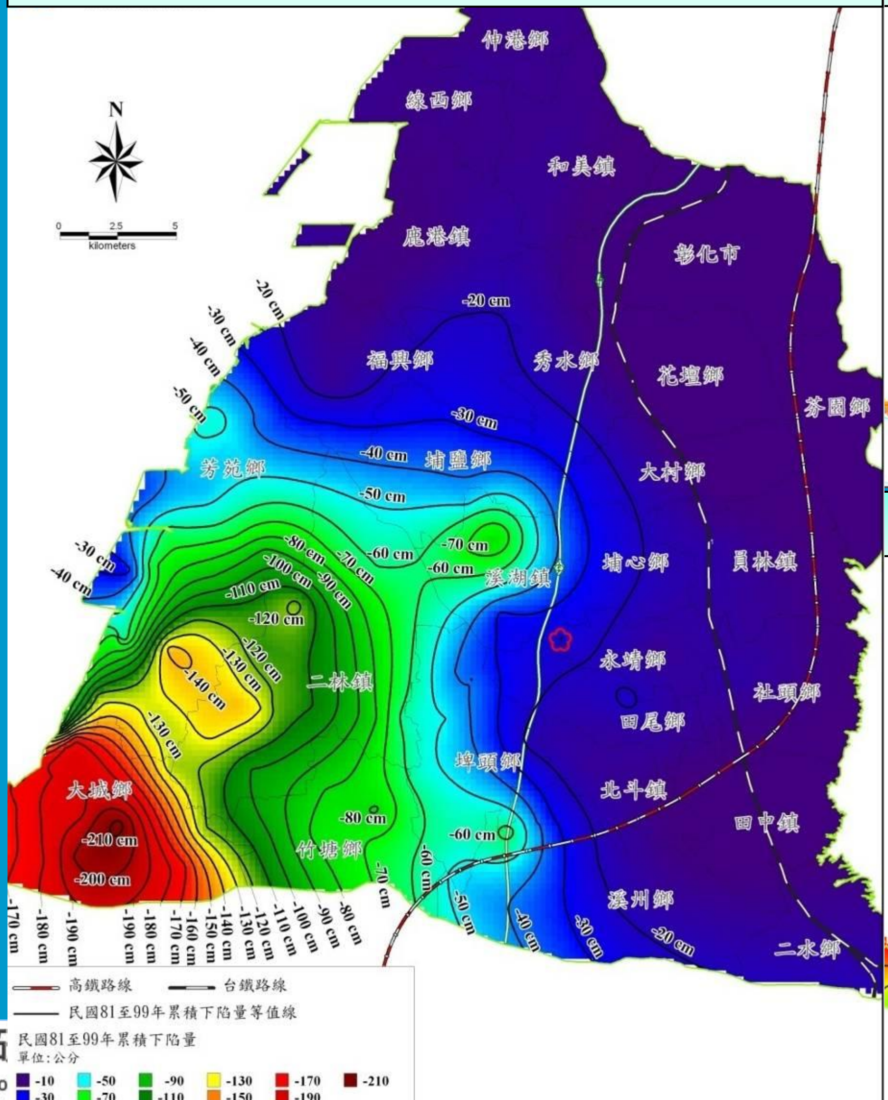

1992-2001

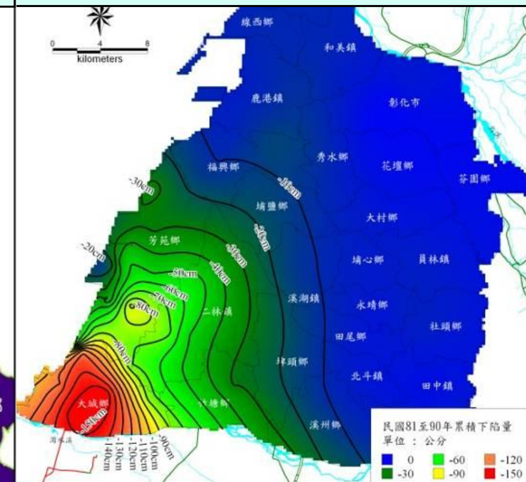

2001-2010

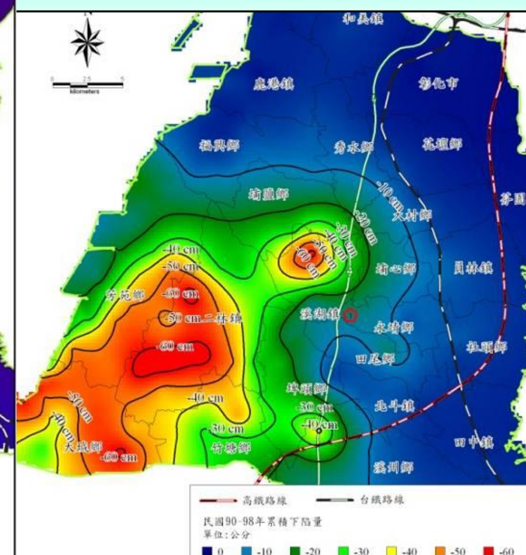

工業技術
Industrial Technolo
Research Institute

Cumulative subsidence in Yunlin County from 1992 to 2010

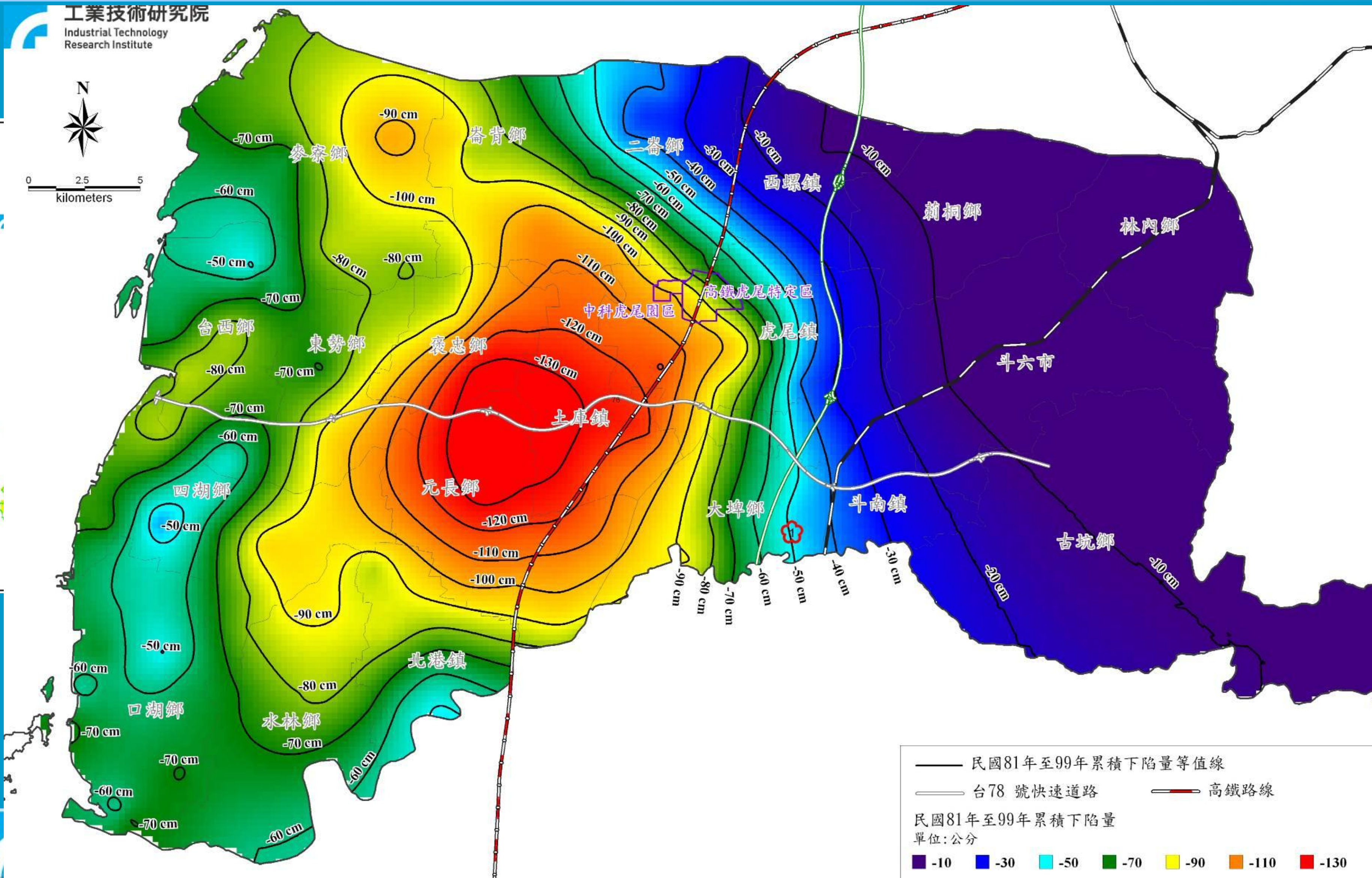

Choushui River Alluvial Fan(CRAF)

1.Fine-granted sediment 2. Groundwater variation

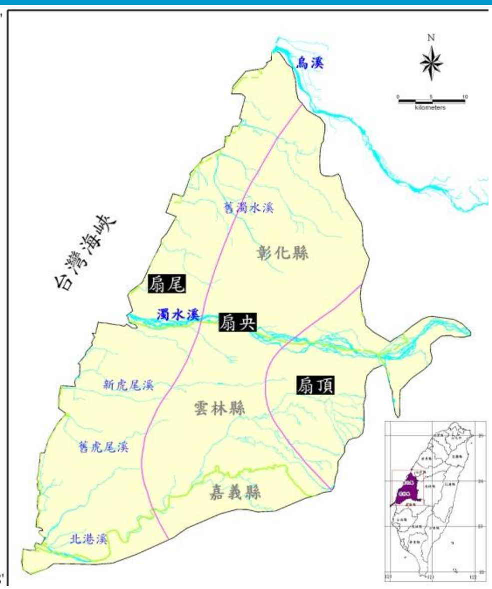

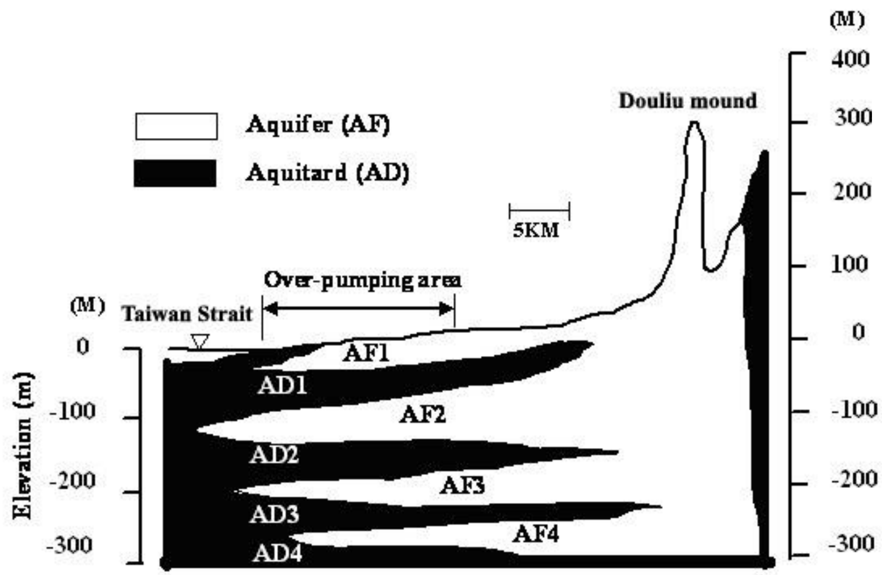

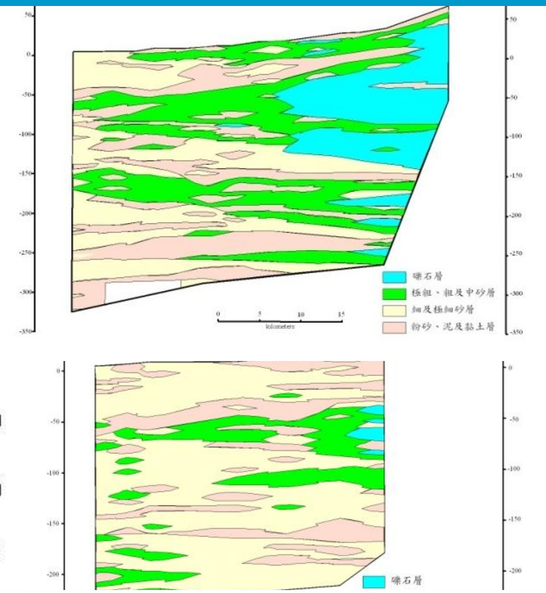

位置	主要土壤組成	壓縮潛能
扇頂	礫石及粗砂	低
扇央	介於扇頂與扇尾之間	高（速度快）
扇尾	細砂及黏土	高（速度慢）

壓縮潛能差異說明

粗顆粒土壤，具有高強度及高透水性，不僅可壓縮性低，且容易獲得地表水之補注，因此地層下陷的潛能低。

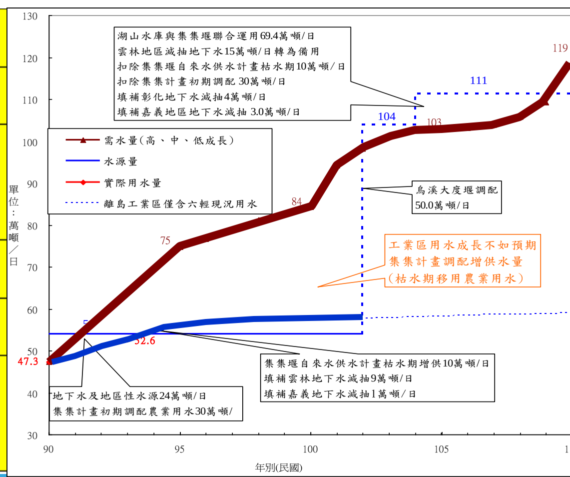

縣市	調查年度	水井調查口數	地下水有效水權		違法水井粗估口數
			水權狀	臨用用水	
宜蘭縣	82	15,177	316	6	14,855
台北市	61	966	11	0	955
新竹縣	83	1,761	364	0	1,397
新竹市	83	774	106	0	668
苗栗縣	83	8,608	348	0	8,260
彰化縣	～98	69,913	1,447	1	68,465
雲林縣	~ 96	107,689	1,725	67	105,897
嘉義縣	~ 97	34,560	5,083	13	29,464
嘉義市	80	540	86	0	454
台南市	80	1,201	38	0	1,163
台南縣	~ 97	24,462	641	107	23,714
高雄縣	~ 97	17,683	1,342	10	16,331
高雄市	80	2,439	350	13	2,076
屏東縣	~ 97	17,711	5,460	38	12,213
		303,484	17,317	255	285,912

2. Synergy of monitoring sensors

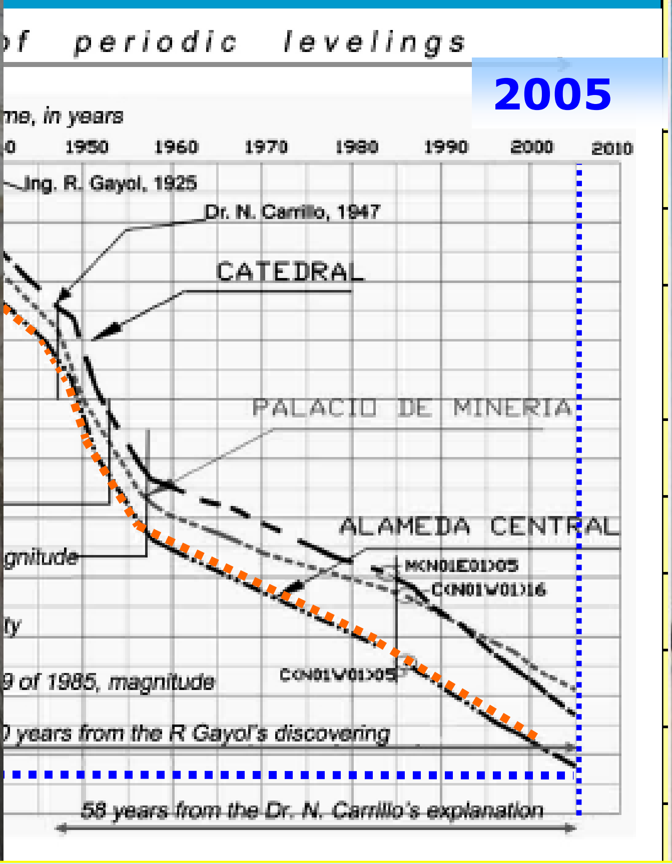

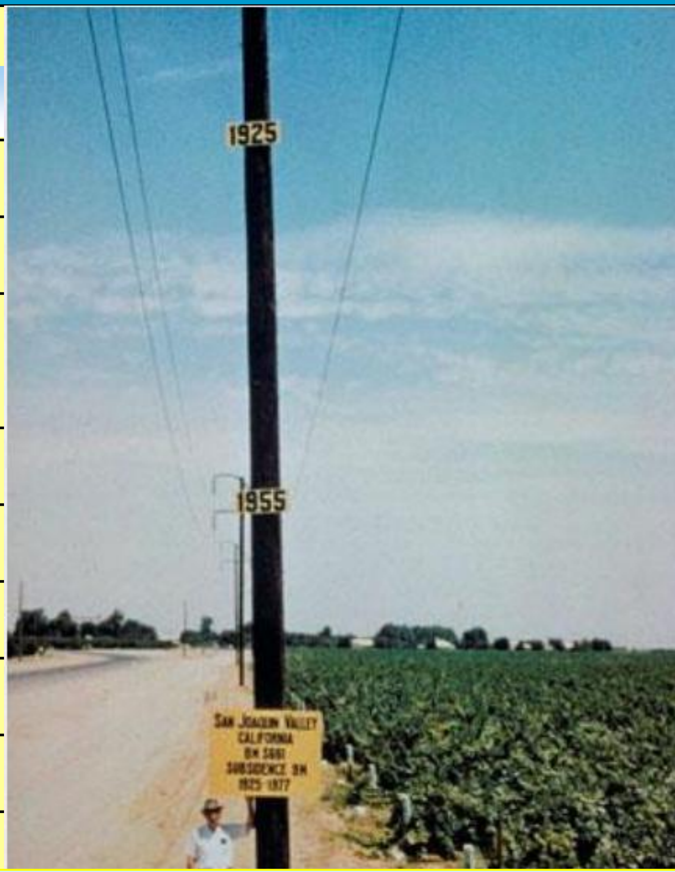

To **integrate** the land subsidence information obtained by **geodesy, geo-hydrological and geo-technical measurements** to achieve a **better understanding and modeling** of land subsidence phenomena.

Multi-Sensors Monitoring System

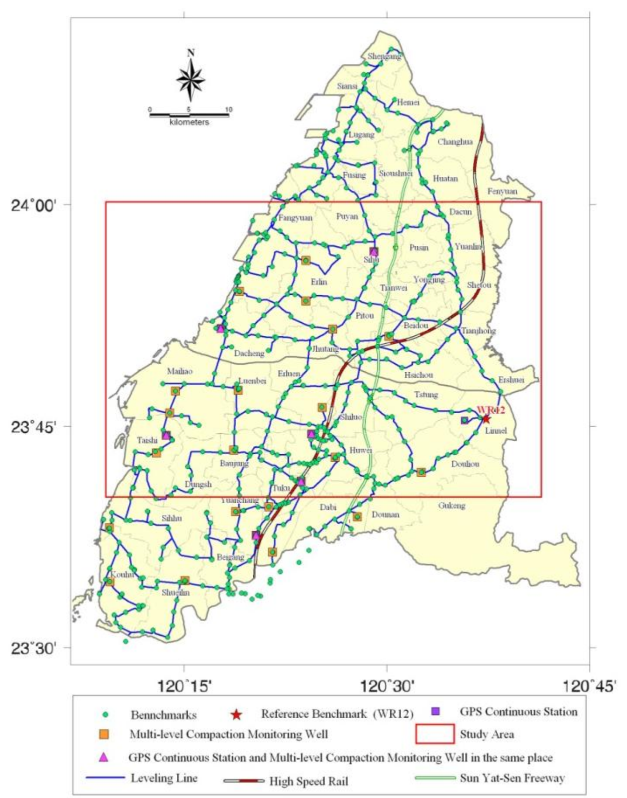

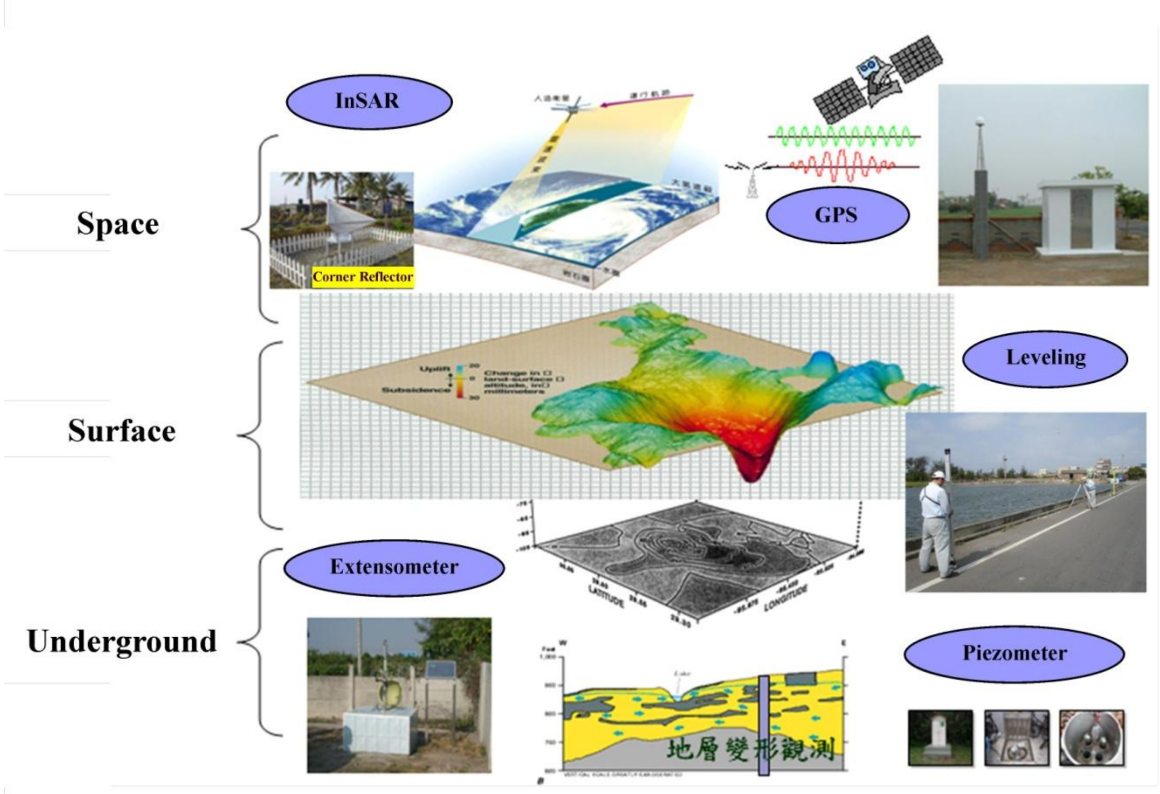

	Spatial Resolution	Measurement Frequency	Measurement (Vertical) Accuracy
Leveling	1.5 - 2 km	1 year	0.5 - 1 cm
Continuous GPS	10 - 15 km	1 day	05 - 1 cm
Monitoring Well	5 - 10 km	1 month	0.1 - 0.5 cm
DInSAR	25 m	35 days	2 cm

Multi-Sensors Monitoring System in Taiwan

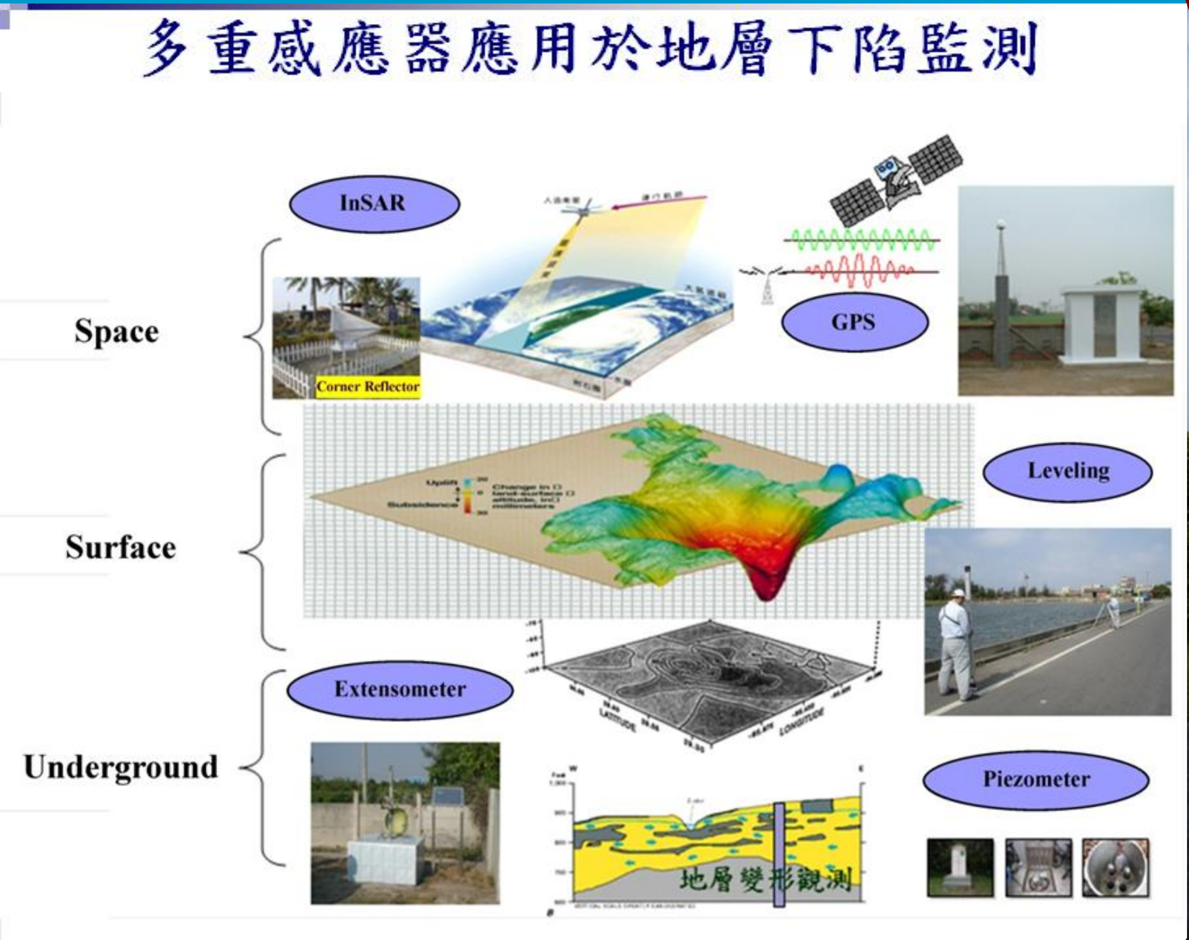

Distributions of Leveling Benchmarks, Monitoring Wells and GPS stations in CRAF

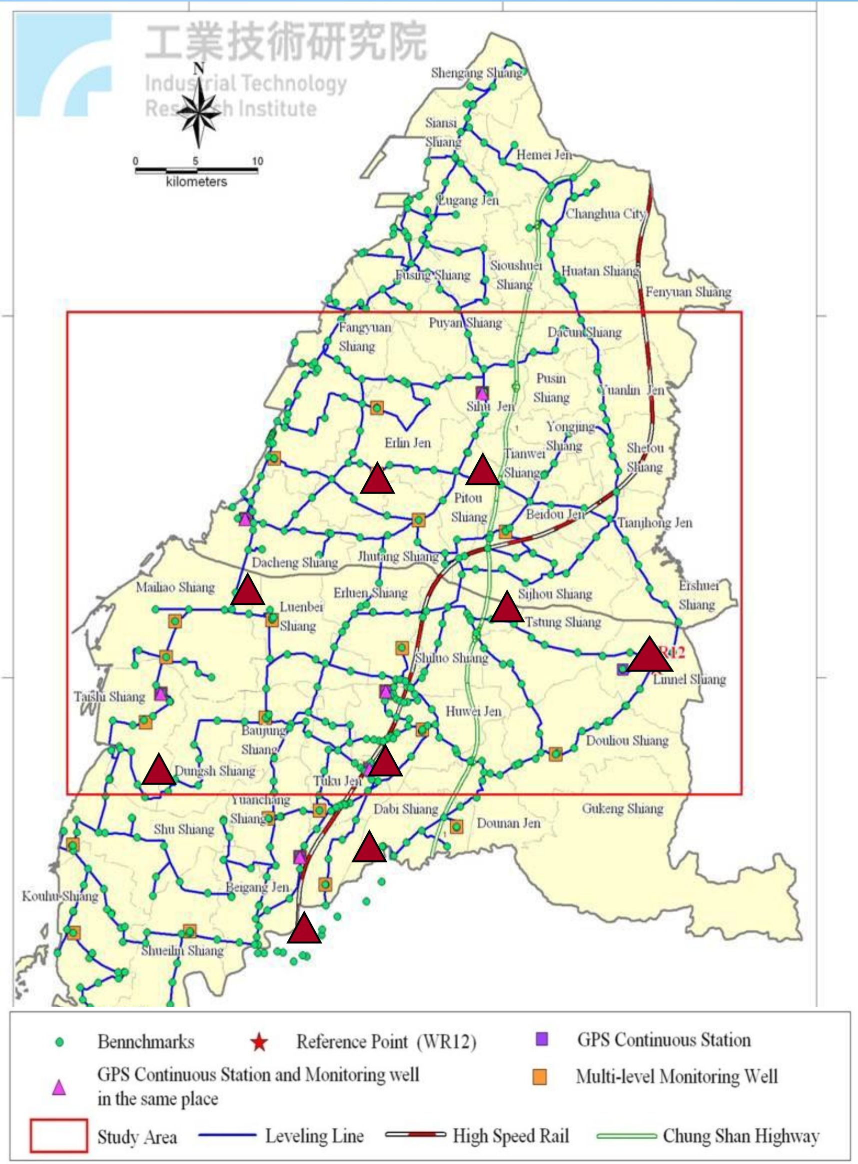

Continuous GPS Station
9 Stations

Leveling Network
850 KM

Multi-layer Compaction Well
29 Wells

Piezometer
108 Wells

GPS Technology Application

GPS


Continuous


Campaign
雲林地區高鐵沿線每2公里一個GPS監測點，共16站


雲林地區GPS監測樁，共11站

Campaign GPS

優點

- 符合NGS58測量規範
- 強制對心
- 架設穩定
- 固定高度(利於測高)
- 樁型穩固,不易破壞遺失
- 佔地面積小,兼具固定站

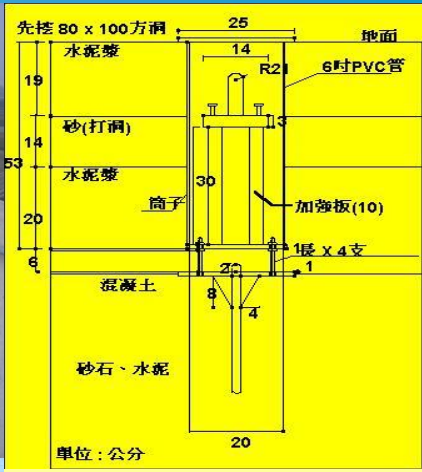

中華民國182781號

新型專利

Traditional Pile Type

New Pile Type

Apply GPS to monitor land deformation

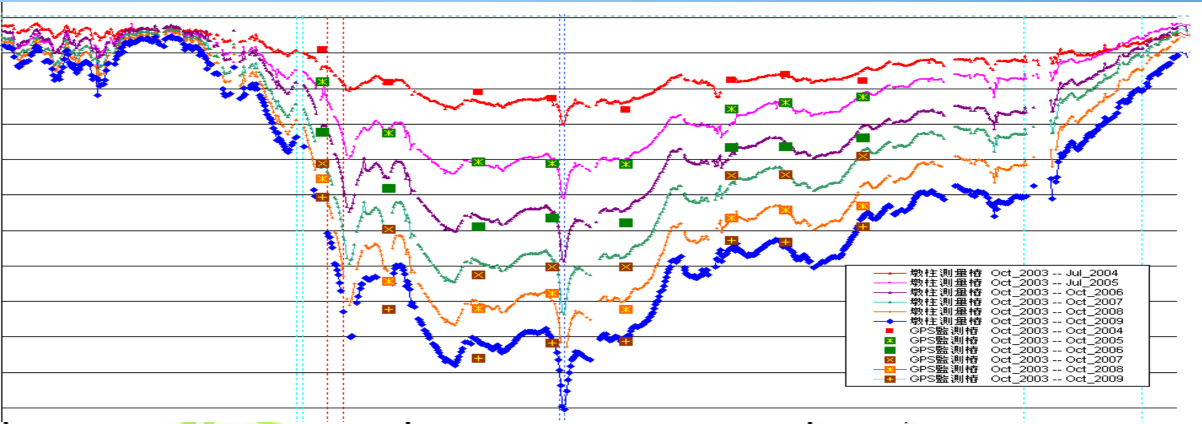

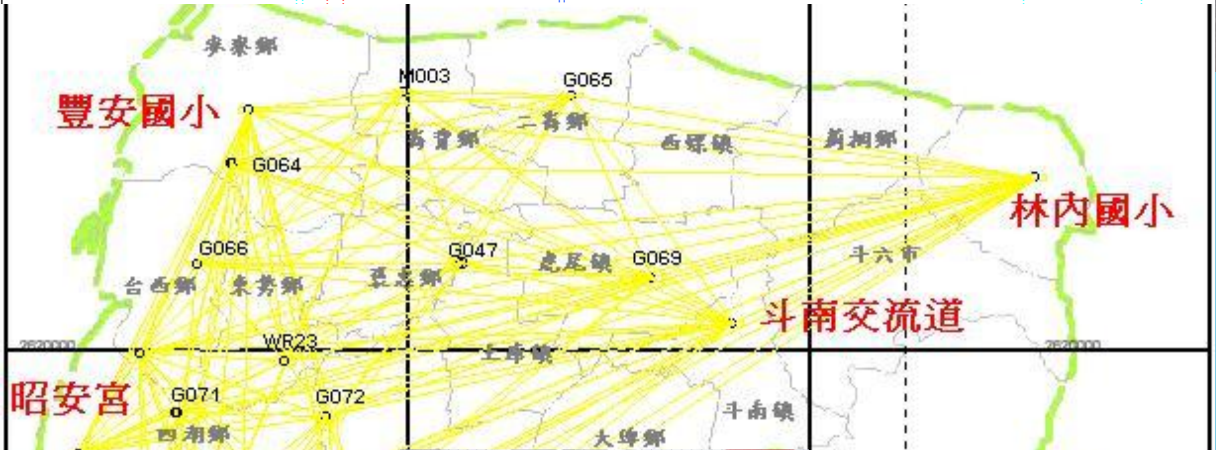

Continuous GPS

標石種類	多路徑效應	穩定性	冷縮熱漲	安裝
混凝土式	高	好	低	固定在岩盤或土壤
深鑽錨式	低	好	非常低	固定在岩盤或土壤
金屬棒外加套筒式	低	好	非常低	固定在岩盤上
NGS套筒式	低	好	非常低	固定在土壤中
不鏽鋼柱式	N/A	好	非常低	固定在岩盤上




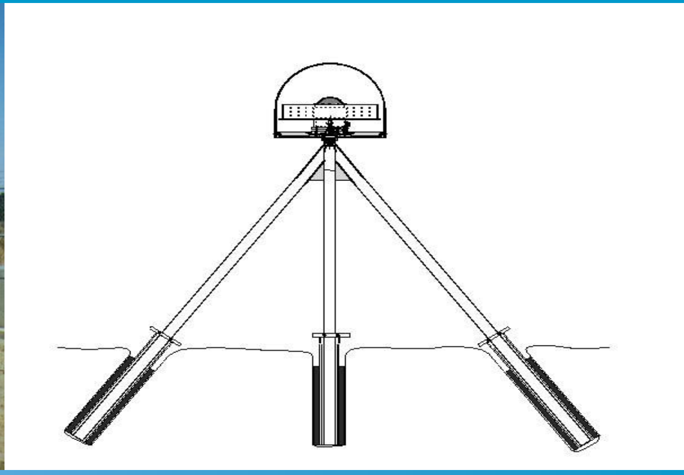

Distribution of Continuous GPS Stations

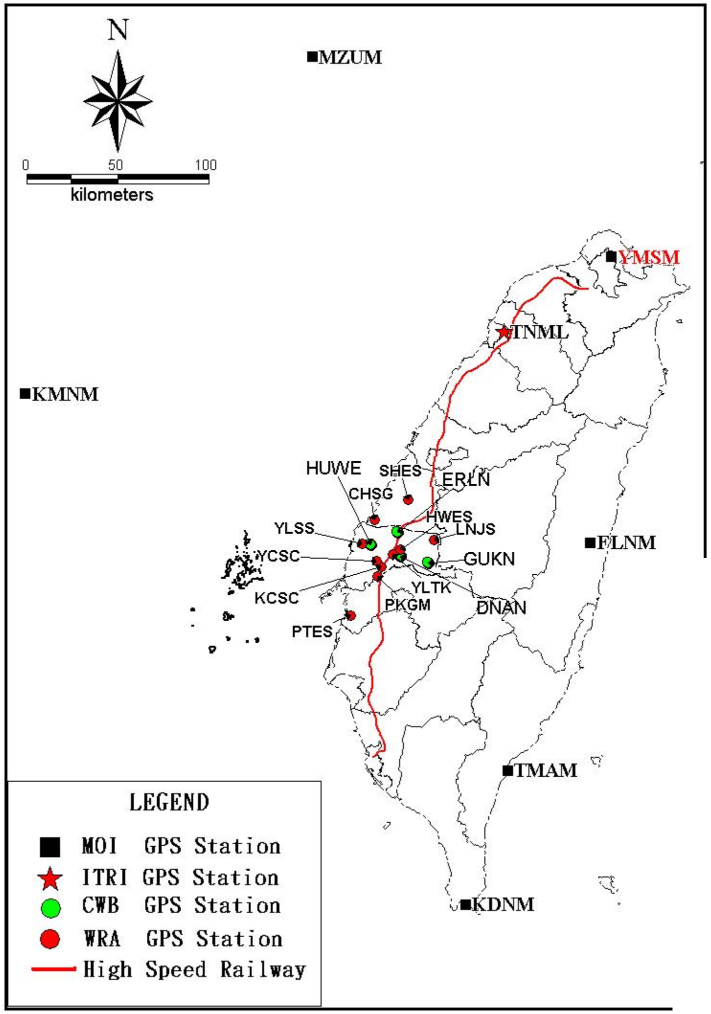

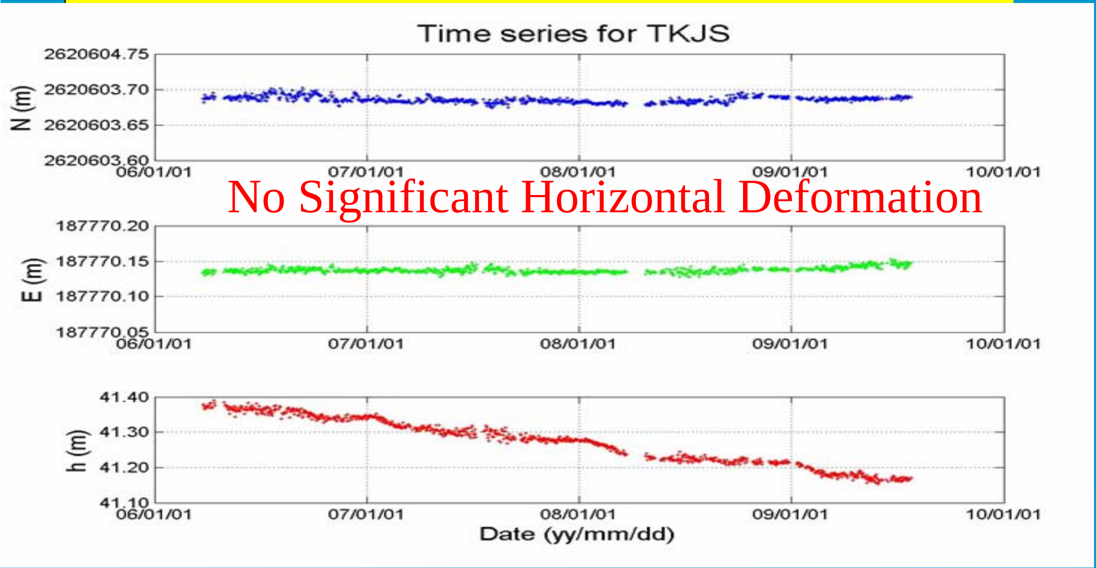

工業技術研究院
Industrial Technology Research Institute

Multi-layer Compaction Monitoring Well

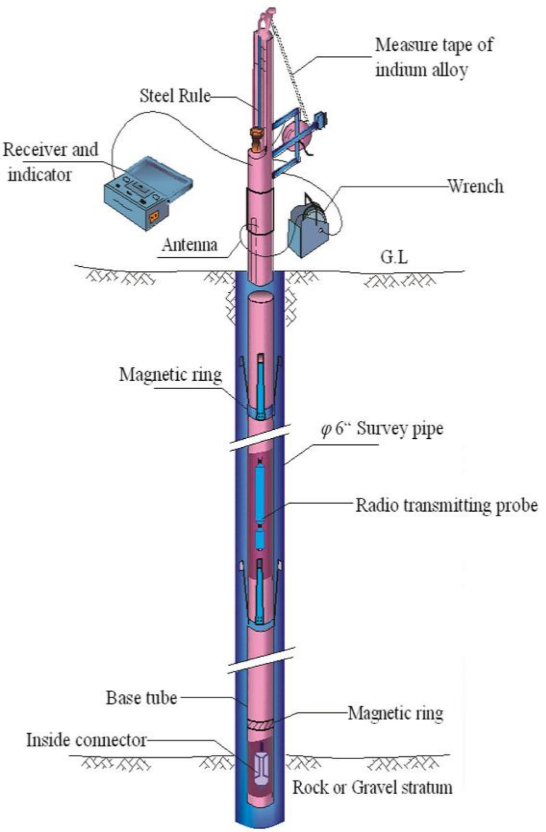

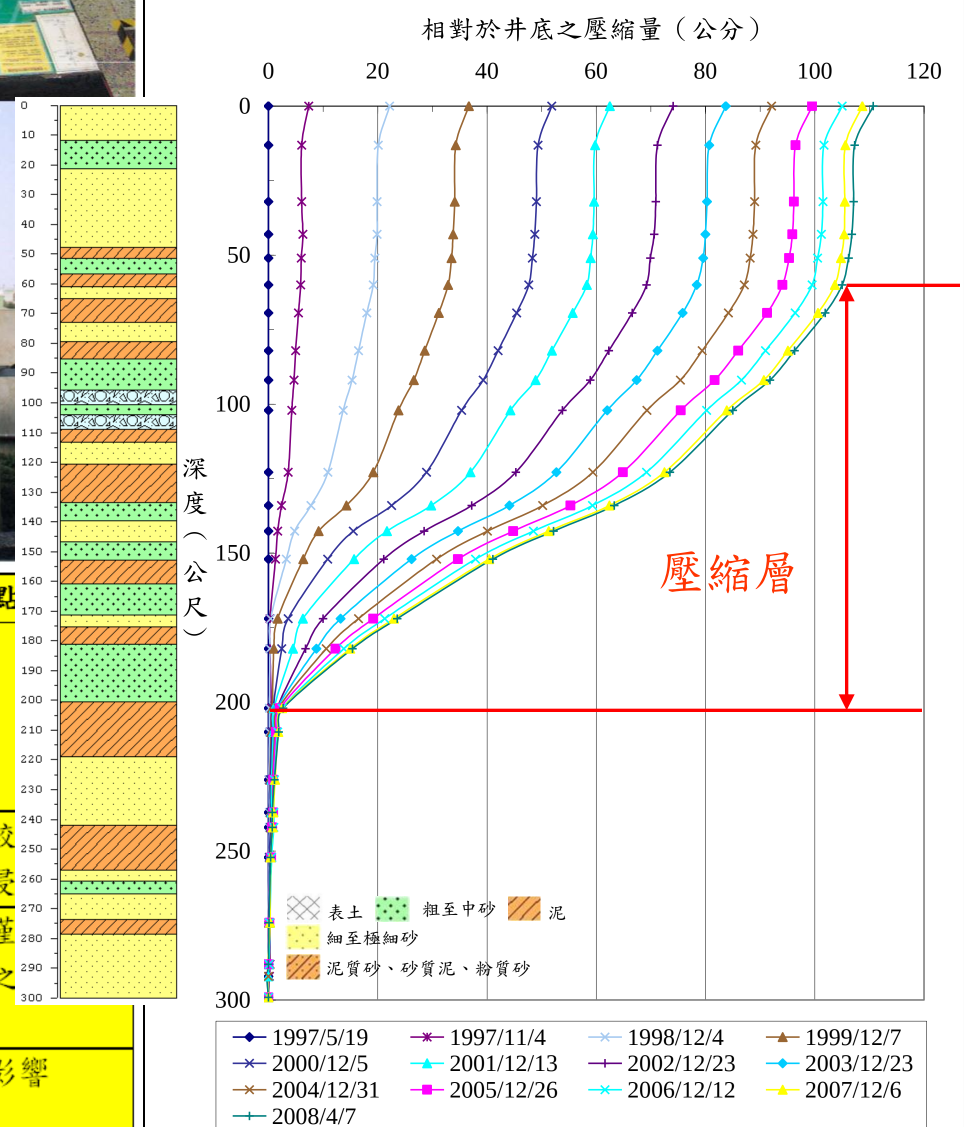

監測井型式	優　　　點	缺
(a)磁環分層式	• 測讀精度高 • 耐久性佳 • 適合大深度量測 • 監測層次具彈性	• 難以自動化量測 • 成本高
(b)鋼　索　式	• 簡單且容易設置 • 成本低廉	• 誤差較大，精度較 • 設備較易受鹽化侵
(c)多點伸張式	• 可多層量測 • 量測容易可自動化監測	• 設置過程需非常謹 則極易影響監測之 • 設置成本高
(d)鋼　管　式	• 可自動觀測 • 設置較容易	• 易受地層摩擦力影響 • 僅單層監測

Aquifer-System Compaction in CRAF

地區	區位	監測站名	期距 (民國)	單位厚度壓縮速率(cm/(yr*m))			
				含水層1	含水層2	含水層3	含水層4
彰化	扇央	湖南國小	97/10~98/10	0.00973	0.01303	**0.02242**	—
彰化	扇央	興華國小	97/10~98/10	—	0.02082	0.01645	**0.09479**
彰化	扇尾	新街國小	97/10~98/10	0.00227	0.00440	**0.00842**	0
彰化	扇尾	西港國小	97/10~98/10	**0.01563**	—	0.00485	0
雲林	扇央	虎尾國小	97/10~98/10	0.00699	0.00866	**0.01540**	**0.01558**
雲林	扇央	土庫國中	97/10~98/10	0.01176	0.01545	0.02326	**0.03003**
雲林	扇央	客厝國小	97/10~98/10	0.01351	0.00585	0.01026	**0.02408**
雲林	扇央	元長國小	97/10~98/10	**0.02414**	0.02366	0.01493	0.01728
雲林	扇尾	龍岩國小	97/10~98/10	0.01308	**0.01957**	0.01574	*
雲林	扇尾	豐安國小	97/10~98/10	0.00250	0.00794	**0.01130**	0.00506
雲林	扇尾	新興國小	97/10~98/10	0.01818	0.01410	0.01667	**0.03404**

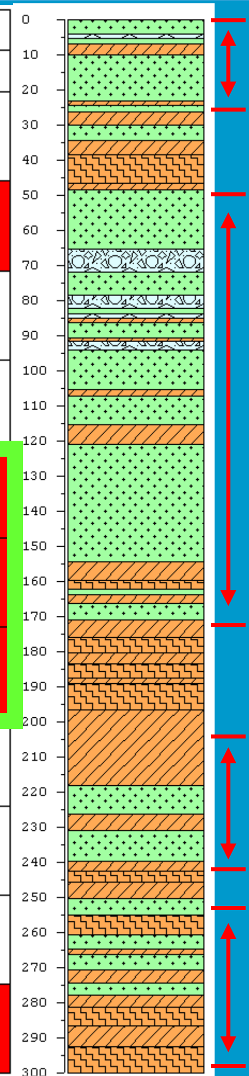

$$\frac{\Delta h_1}{dS_1} = V_1$$

$$\frac{\Delta h_2}{dS_2} = V_2$$

$$\frac{\Delta h_3}{dS_3} = V_3$$

$$\frac{\Delta h_4}{dS_4} = V_4$$

△h： 壓縮量
dS ： 含水層厚度
V ： 含水層單位厚度壓縮速率 (cm/(yr*m))

工業技術研究院
Industrial Technology Research Institute

Comparison between Multi-Sensors System

時　間	水準測量 單位：公分	監測井測量 單位：公分	GPS 測量 單位：公分
90.08~92.07	19.4	19.5	18.6
92.07~93.07	8.8	8.9	8.6
93.07~94.05	7.4	7	6.6
94.05~95.10	8.9	8.6	9.7
95.10~96.07	4.3	4.2	4.5
96.07~97.06	2.6	2.1	2.3
97.06~98.07	1.3(回彈)	0.3(回彈)	0.6(回彈)
98.07~99.05	0.2	0.8	0.7
累　計	50.3	49.8	50.2

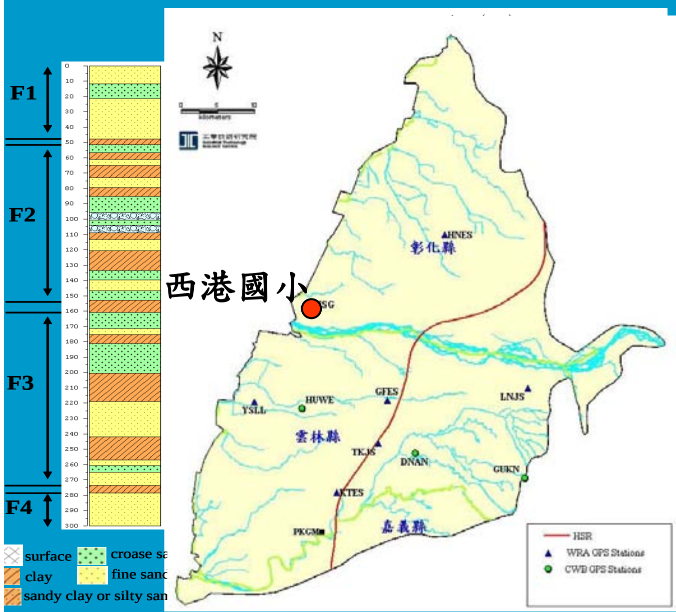

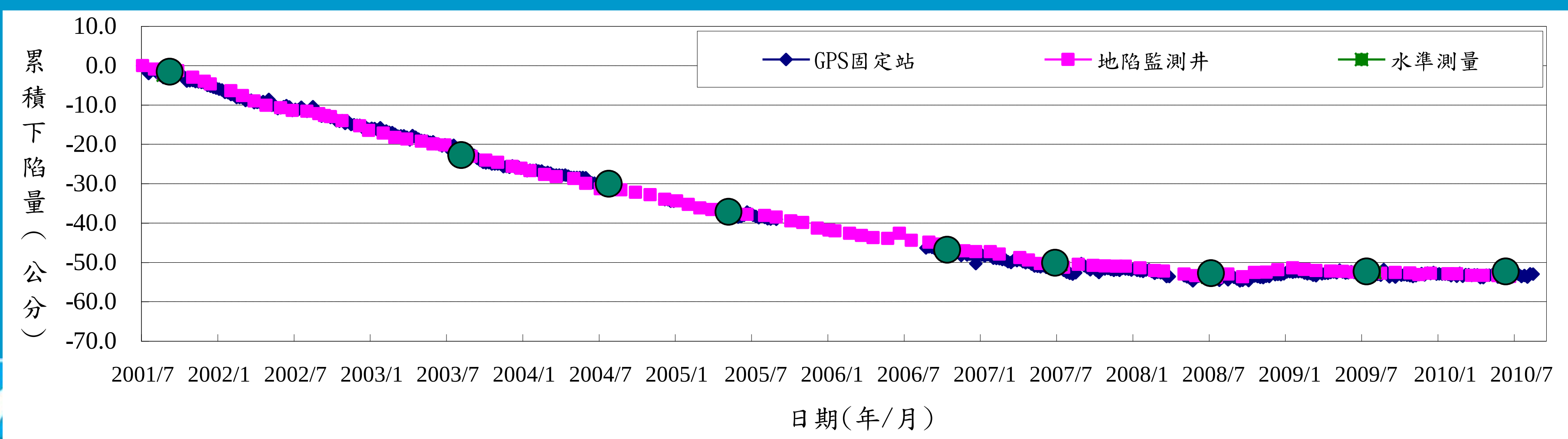

Modeling Aquifer-System Compaction and Predicting Land Subsidence

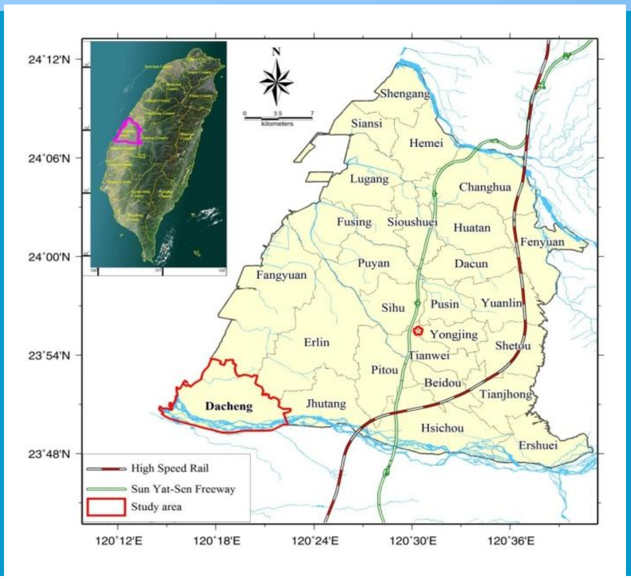

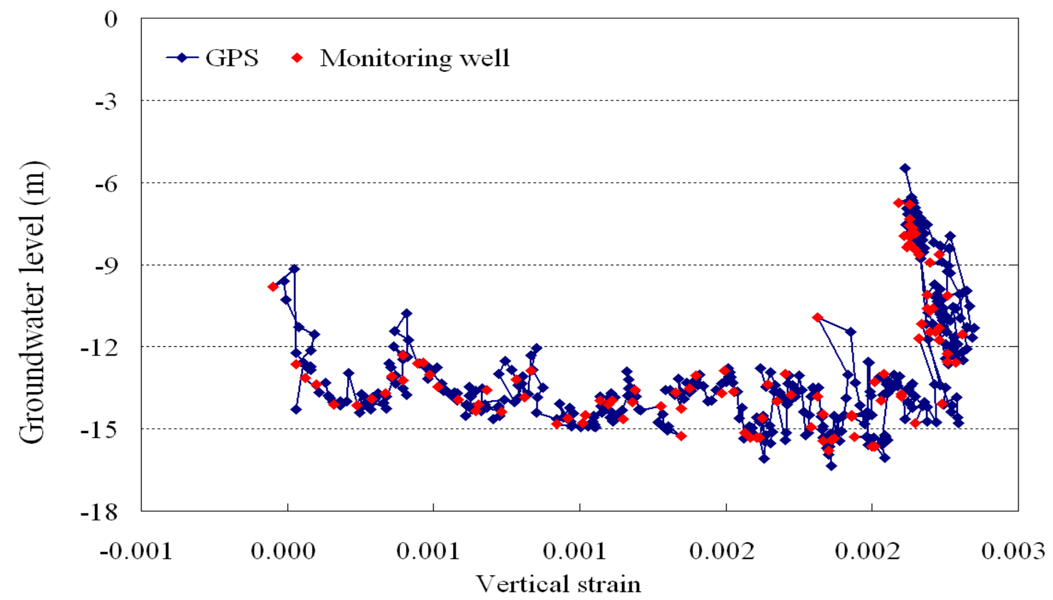

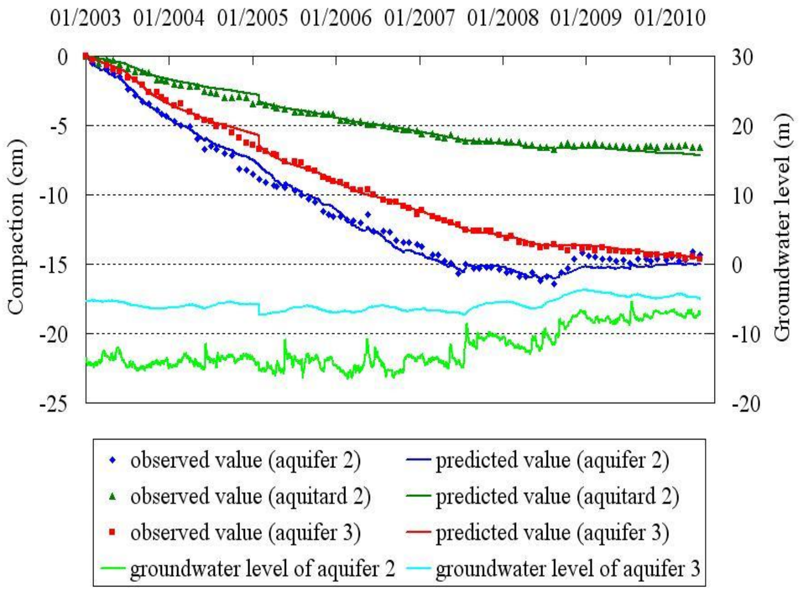

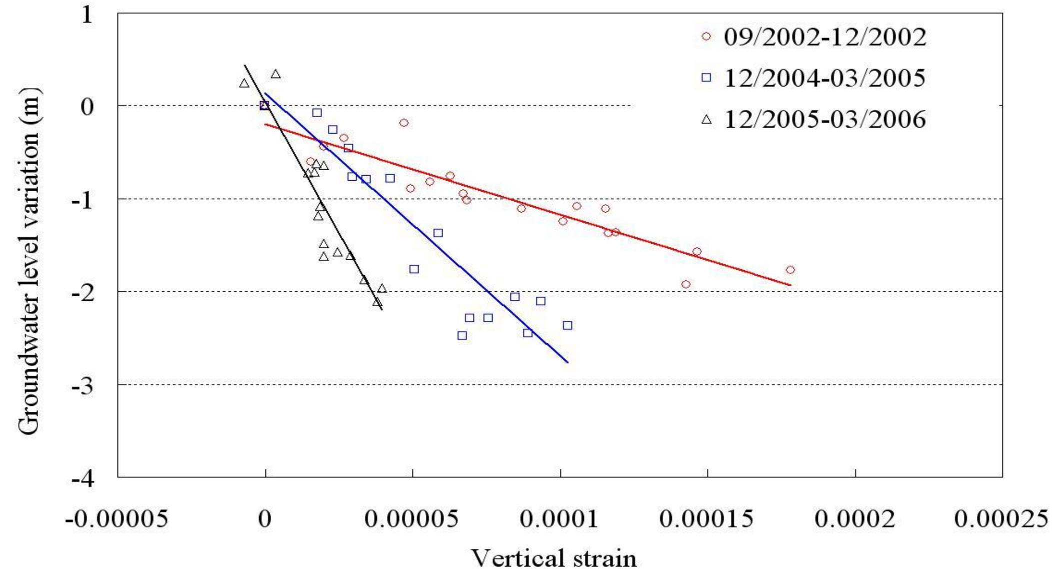

Subsidence Analysis in Yunlin County

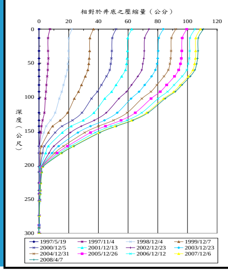

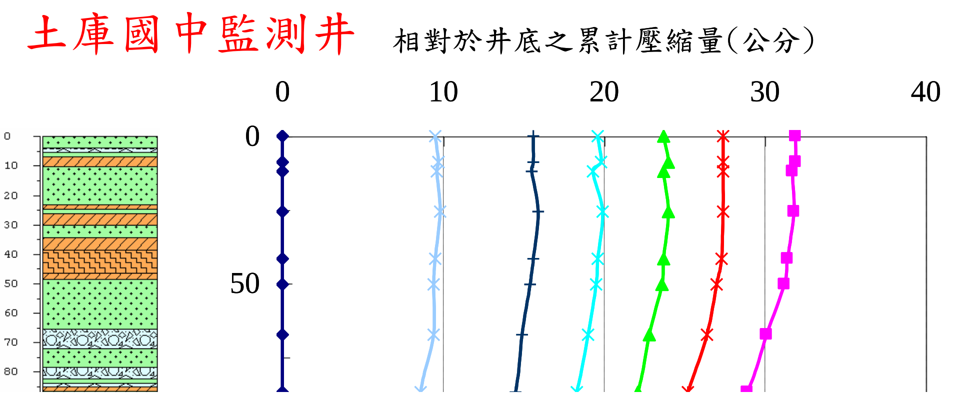

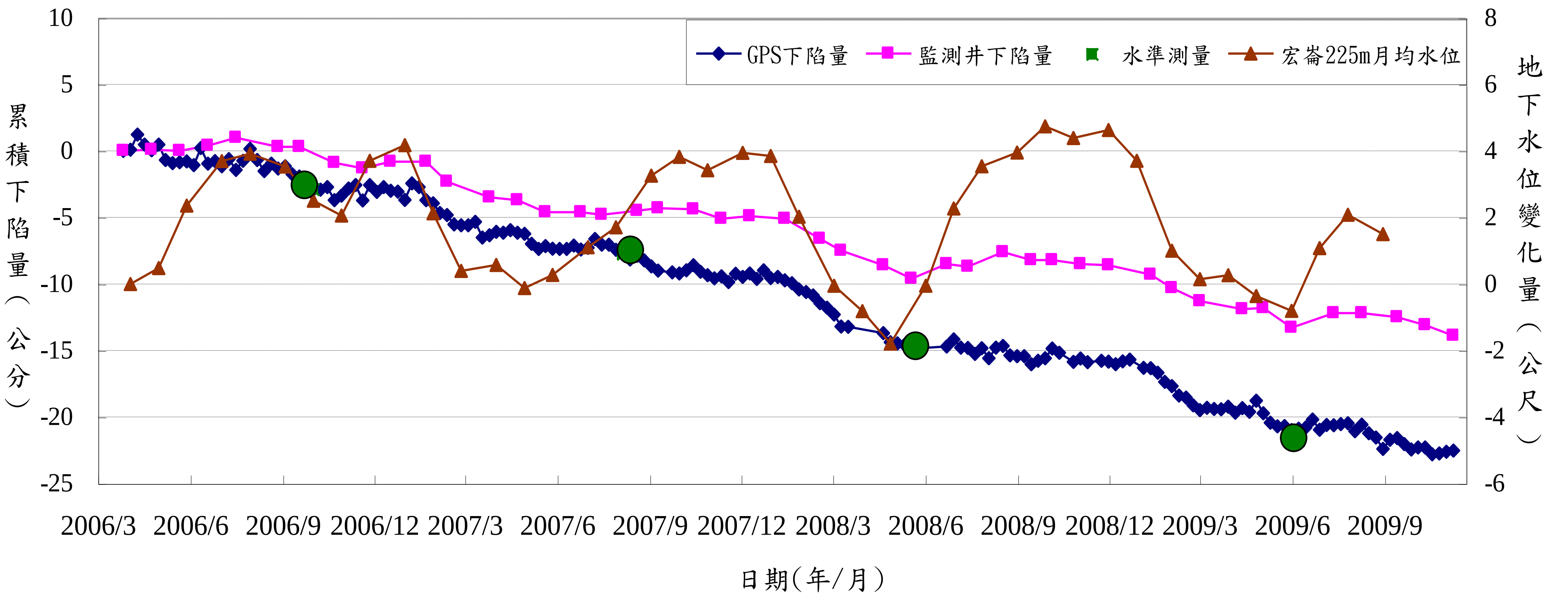

Aquifer Compaction Deeper than 300 m

△H_1＝△h_2＞△H_3：
代表300公尺以下仍有壓縮

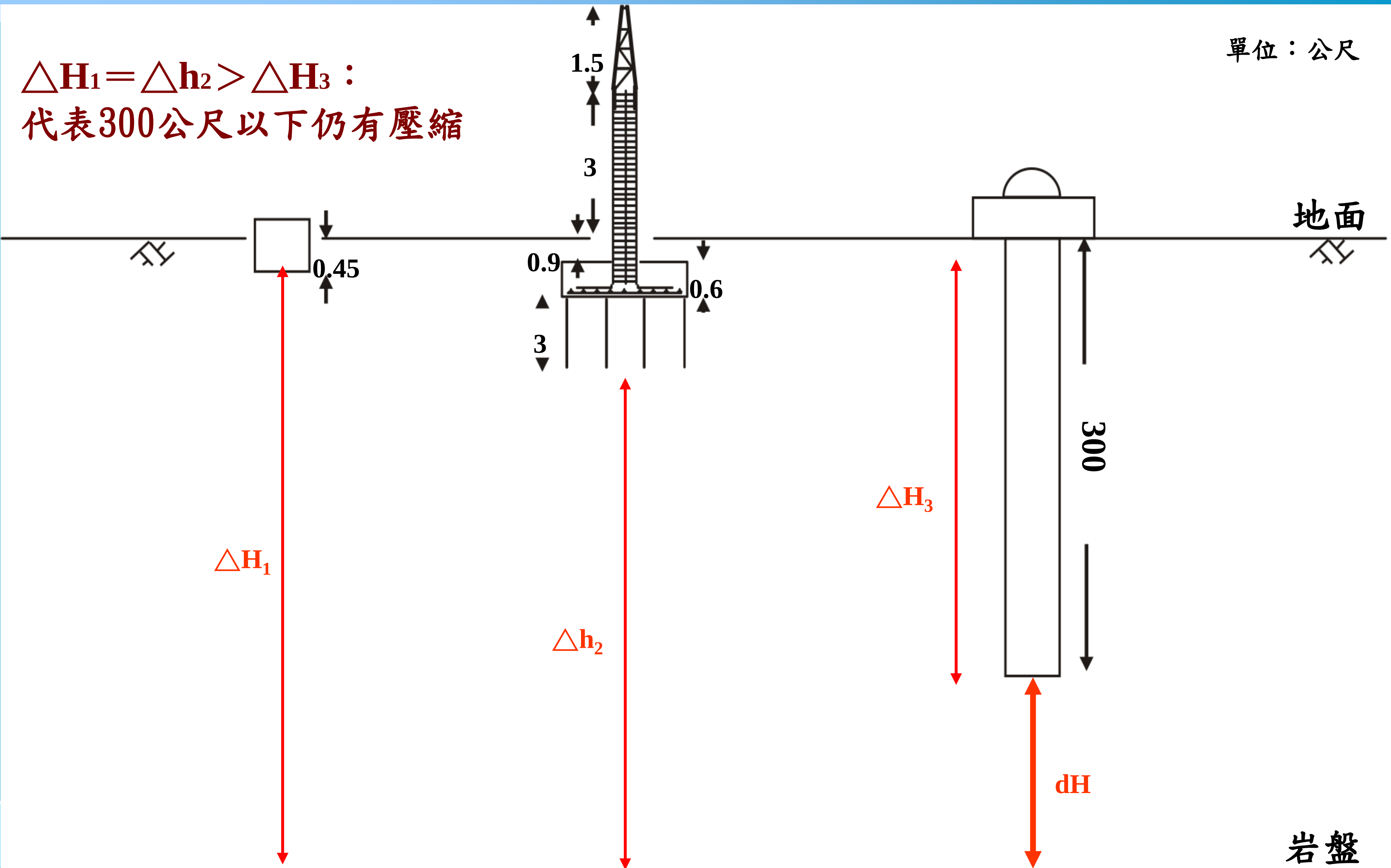

壓縮量分析圖

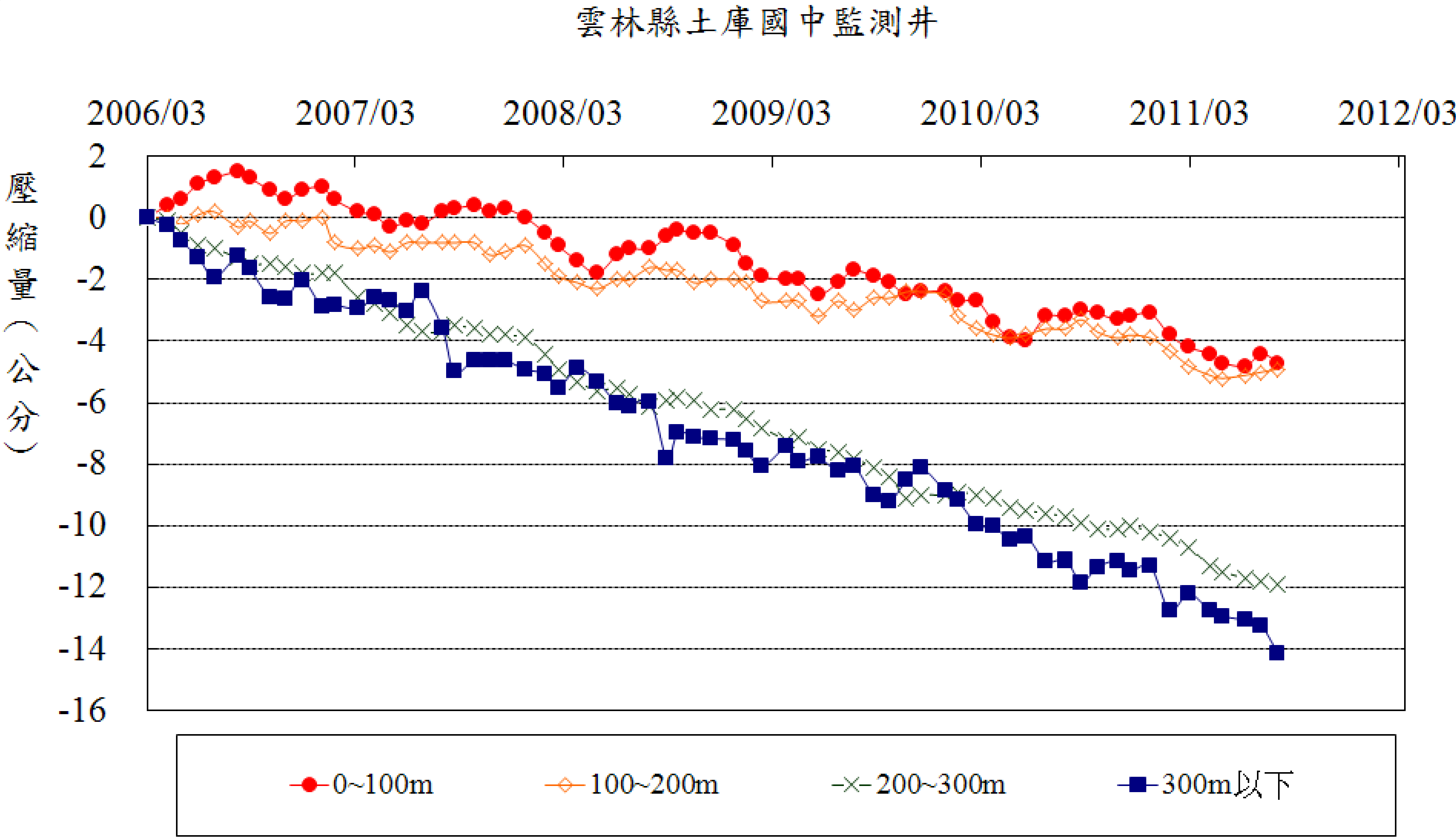
雲林縣土庫國中監測井
2006/03
2007/03
2008/03
2009/03
2010/03
2011/03
2012/03
壓縮量（公分）
2
0
-2
-4
-6
-8
-10
-12
-14
-16
0~100m
100~200m
200~300m
300m以下

Land Gravity Observation and Network

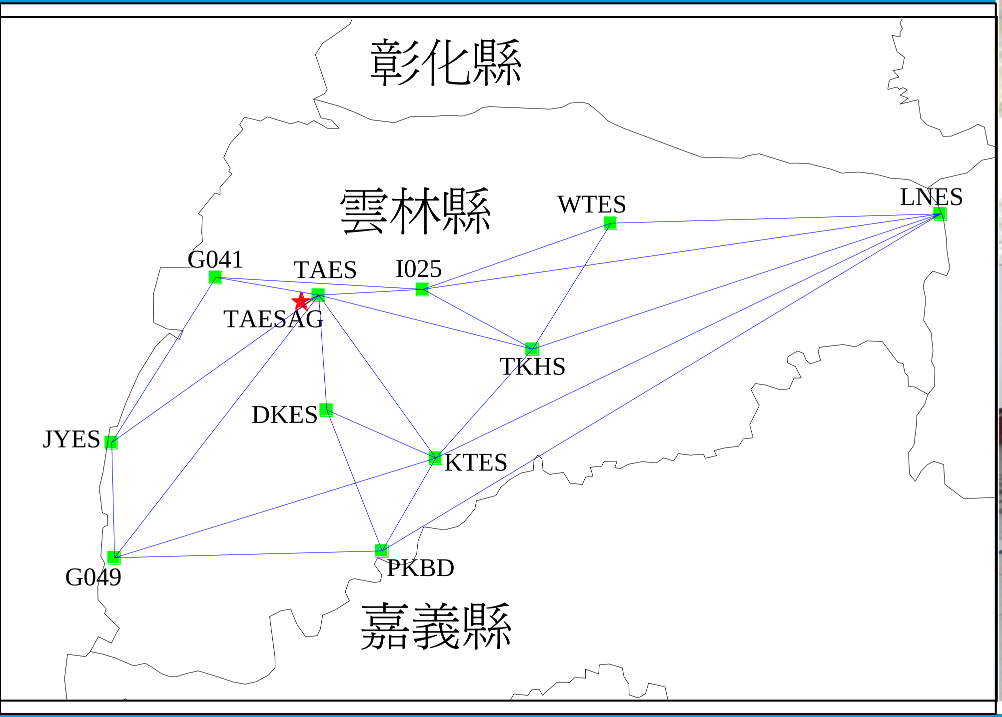

The Necessity of INSAR

過去監測方法：點→線→面

現在監測方法：面→線→點

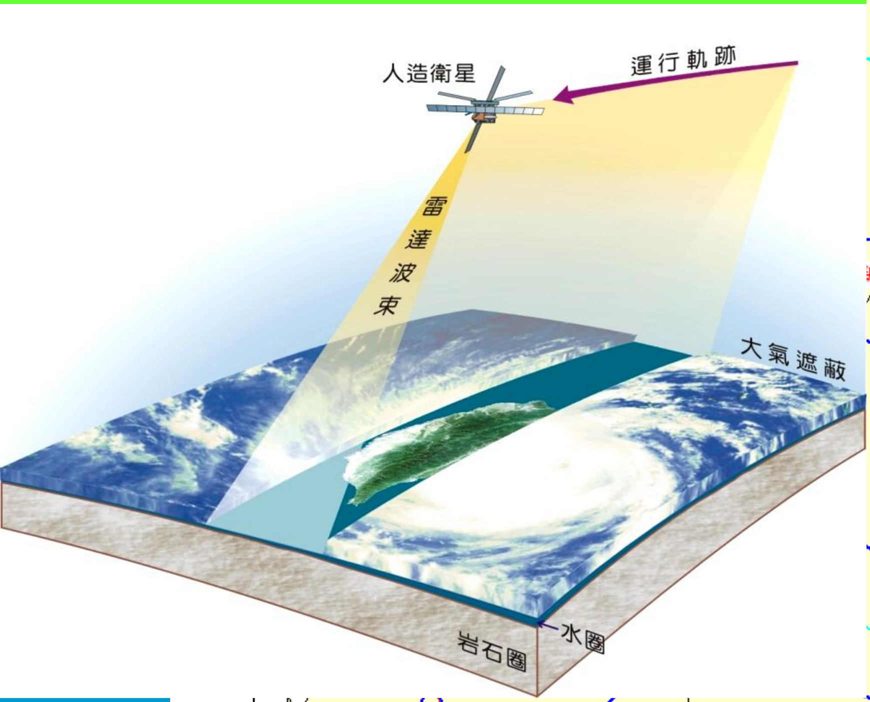

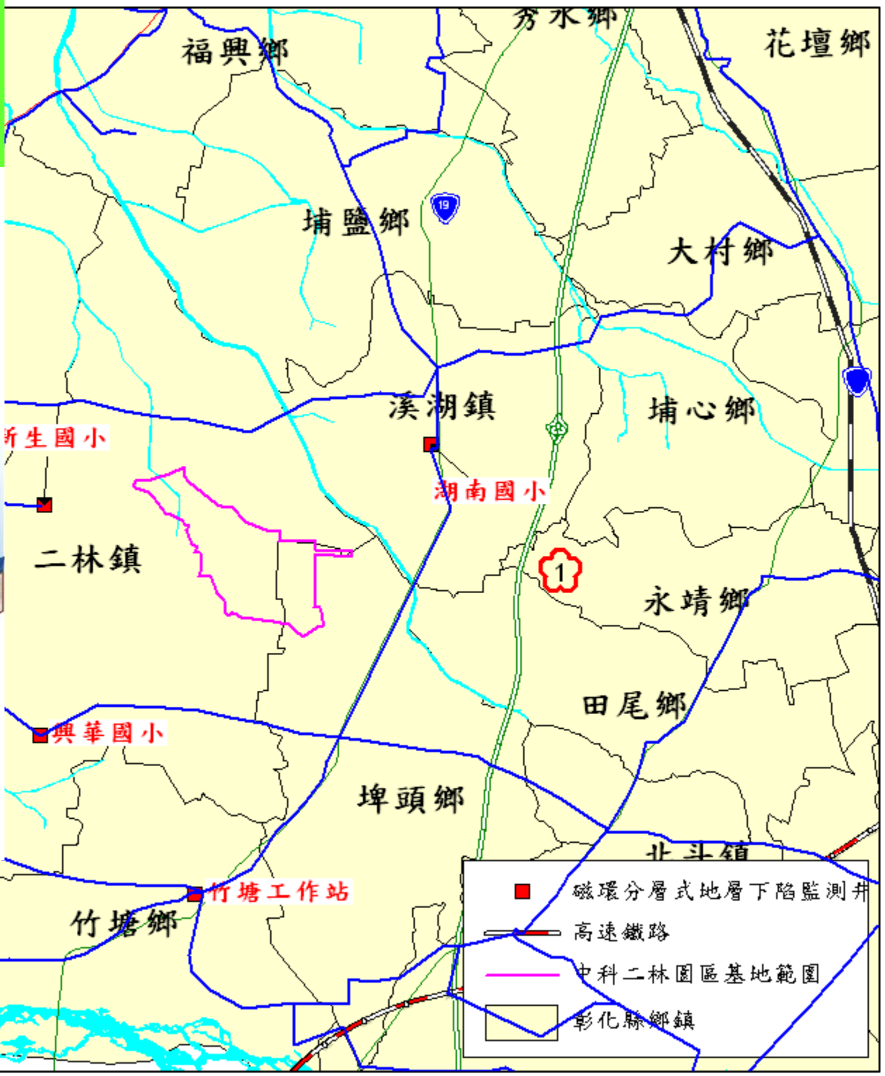

3. InSAR Technique

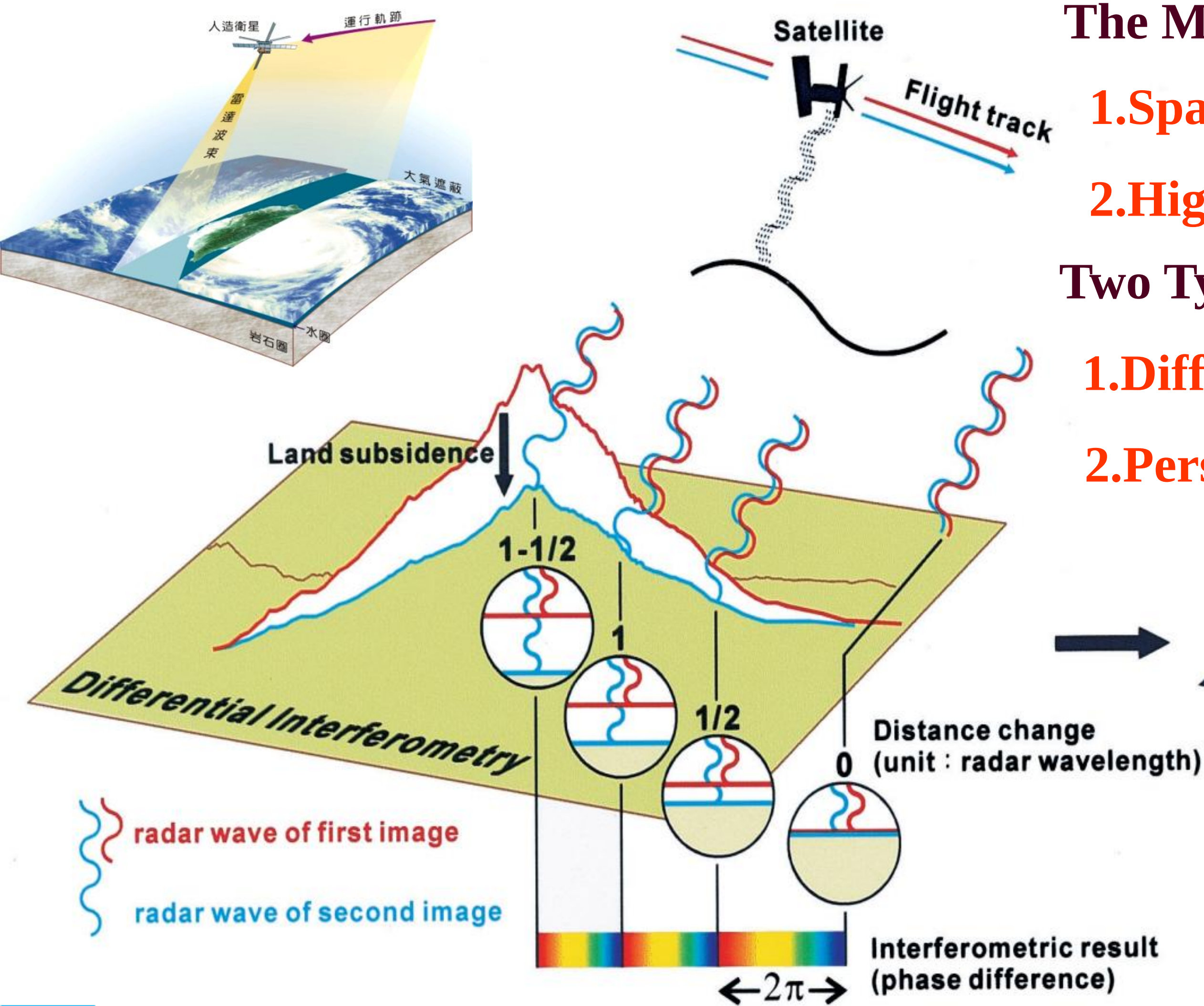

The Major Advantages of InSAR

1.Spacial-wise deformation

2.High accuracy

Two Types of InSAR

1.Differencial InSAR (DInSAR)

2.Persistent Scatterer InSAR (PSI)

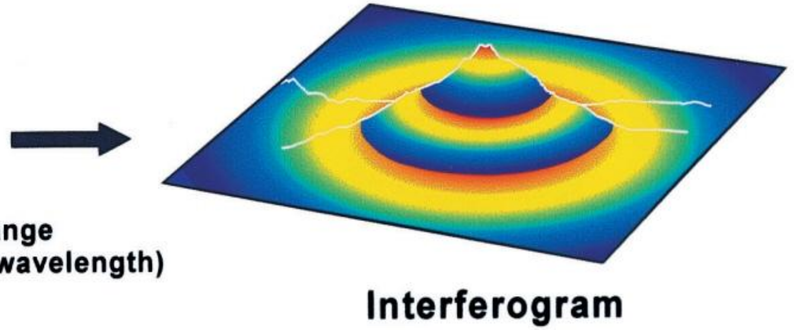

Characteristics and Applications of Civilian Radar Satellites

Satellite Abbreviation	Launch Date	Wavelength (cm)	Band	Orbital Repetition Cycle (days)	Applications
SEASAT	*1978*	*23.5*	*L*	*3*	*Ocean temperature, Wind waves, Hydrology*
ERS-1/2	*1991/1995*	*5.6*	*C*	*35*	*Hydrology, Topographic mapping, Surface deformation detection*
JERS-1	*1992*	*23.5*	*L*	*44*	*Topographic mapping, Land cover and land use mapping, and Environment application*
SIR-C	*1994*	*3.2/ 5.6/ 23.5*	*X/ C/ L*	*variable*	*Topographic mapping, Land cover and land use mapping, Hydrology and Environment application*
RADARSAT	*1995*	*5.6*	*C*	*24*	*Ocean temperature, Hydrology, Topographic mapping, Surface deformation detection*
ENVISAT	*2002*	*5.6*	*C*	*35*	*Atmospheric chemistry, Biological oceanography, Ocean temperature, Wind waves, Hydrology, Agriculture and arboriculture, Natural hazard monitoring*
ALOS	*2003*	*23.5*	*L*	*44*	*Topographic mapping, Surface deformation detection, Land cover and land use mapping, Rapid emergency response and Evironment application*
TerraSAR-X	*2007*	*3.2*	*X*	*11*	

Differential InSAR

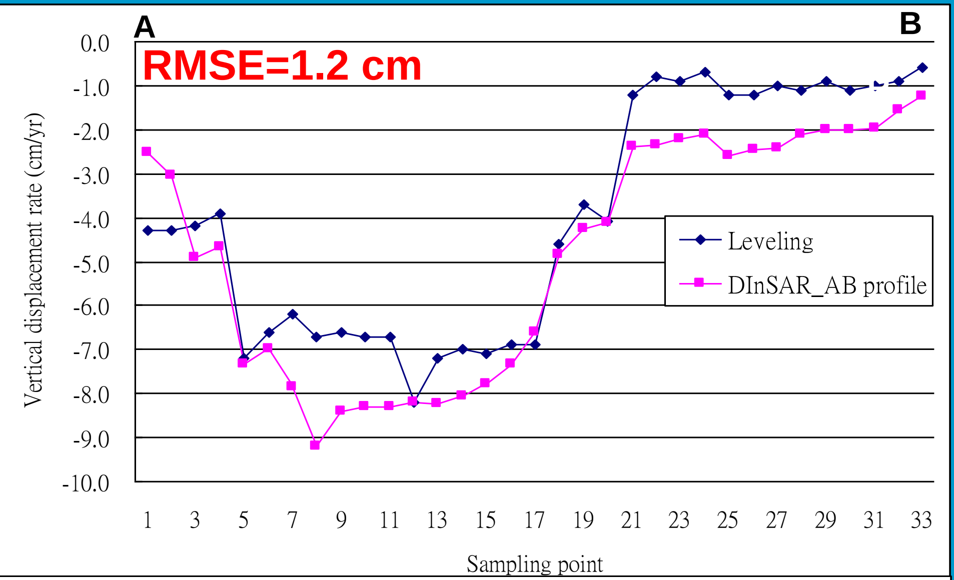

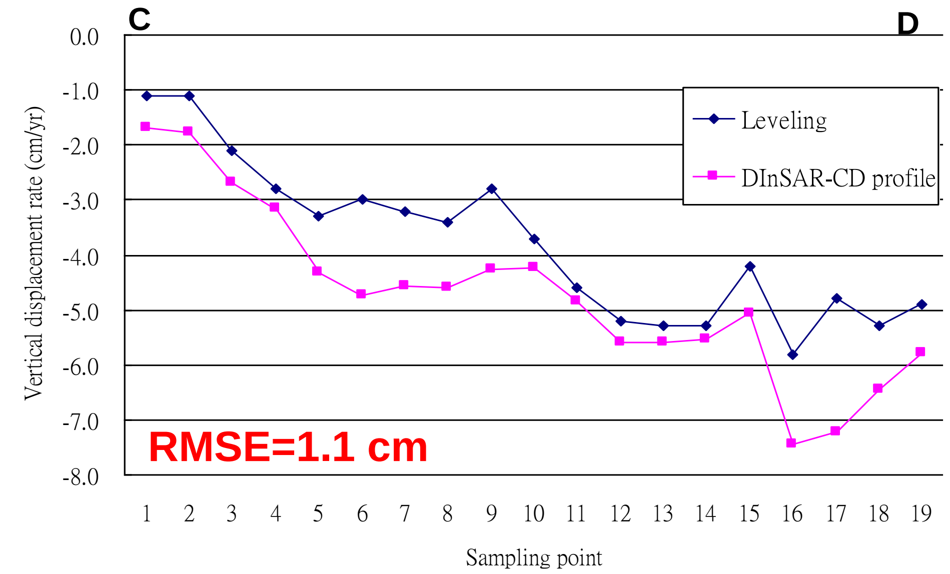

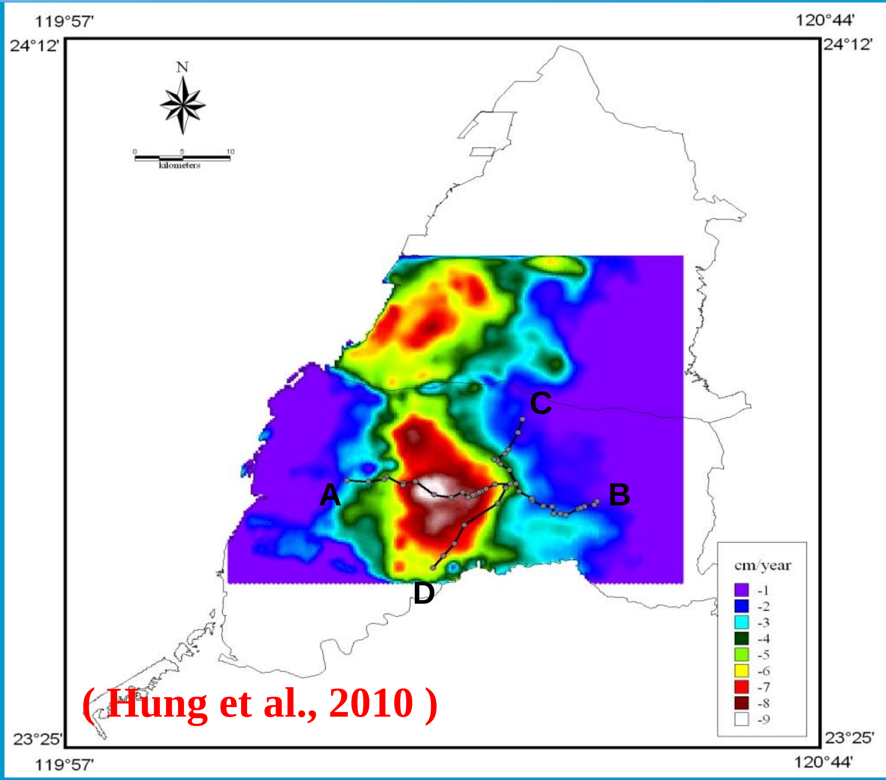

- Many potential errors including **atmospheric heterogeneity** and **phase decorrelation** may degrade the DInSAR result.

- DInSAR has a deficiency in accuracy over coastal areas of CRAF.

Reflect Corner（ITRI）

整體優點

1. 質量輕
2. 耐強風
3. 不積水
4. 360度旋轉
5. 準確調整仰角
6. 適用任何衛星

Persistent Scatterer InSAR
PSI

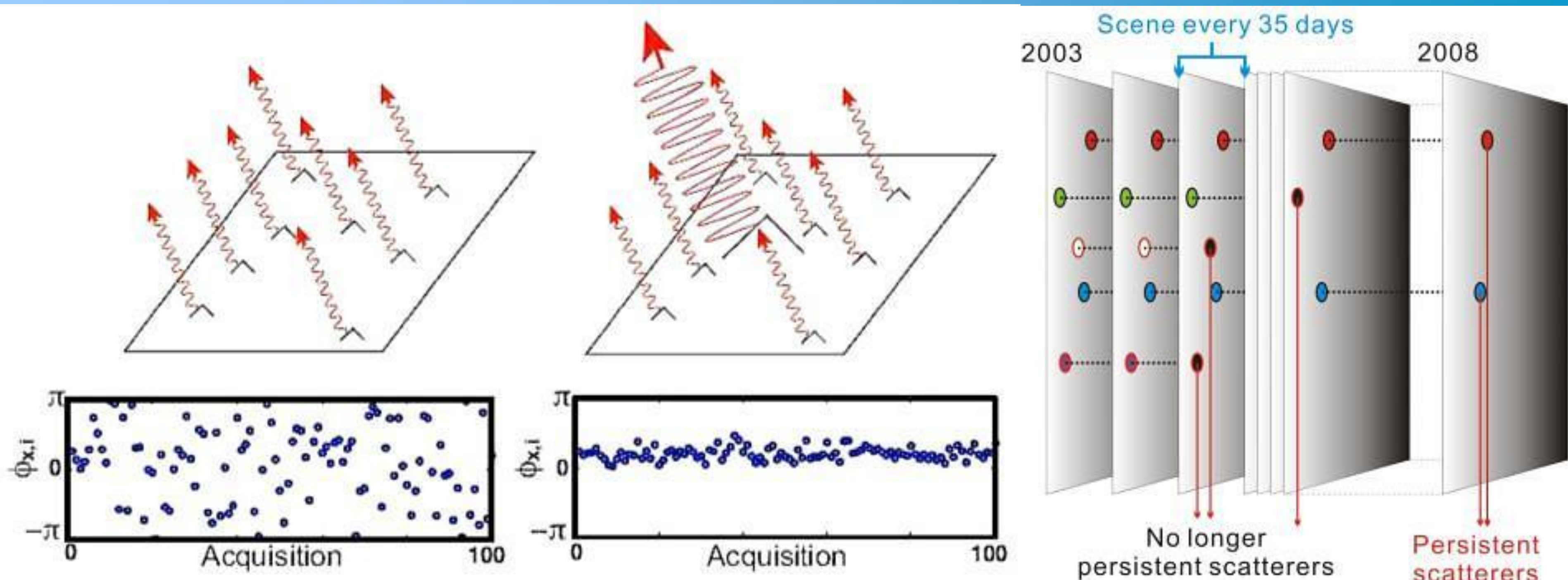

$$\phi_{x,i} = \phi_{def,x,i} + \phi_{\alpha,x,i} + \phi_{orb,x,i} + \phi_{\varepsilon,x,i} + n_{x,i}$$

$\phi_{x,i}$	: interferometric phase	$\phi_{orb,x,i}$	: orbit effect
$\phi_{def,x,i}$	: surface displacement	$\phi_{\varepsilon,x,i}$	: DEM residual effect
$\phi_{\alpha,x,i}$	: atmospheric effect	$n_{x,i}$	: noise

(Ferretti et al., 2000; Hooper et al., 2004)

工業技術研究院
Industrial Technology
Research Institute

StaMPS/MTI Data Process

4 Steps

- DInSAR Process
- PSI Process
- Cross Validation Process
- Fusion Process

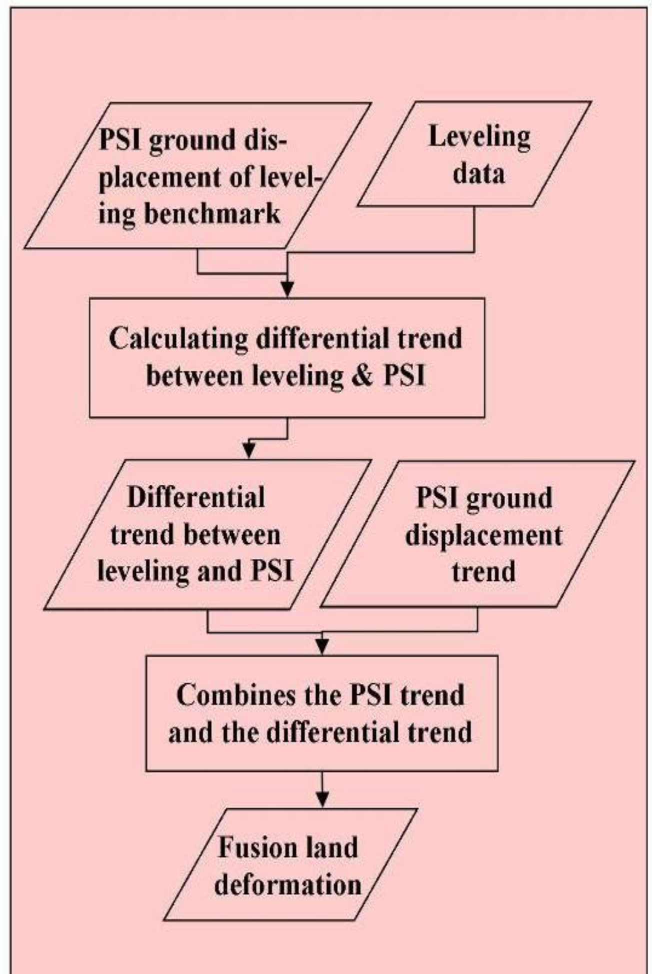

Step.4 Fusion Process

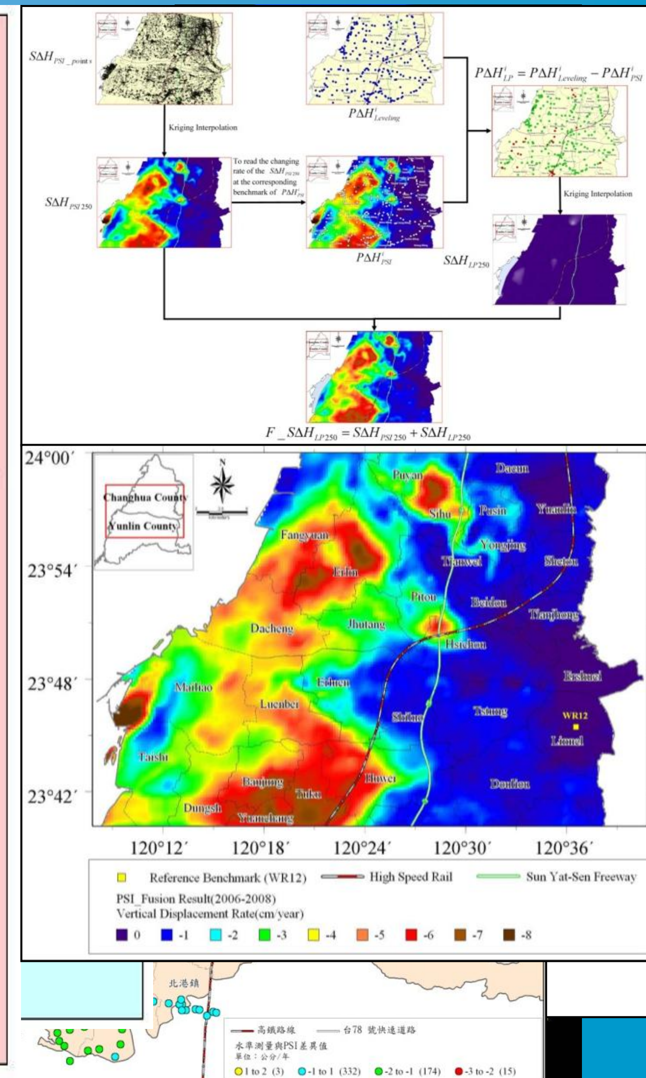

工業技術研究院
Industrial Technology Research Institute

The ... deviation

the ... of the

amplitude value

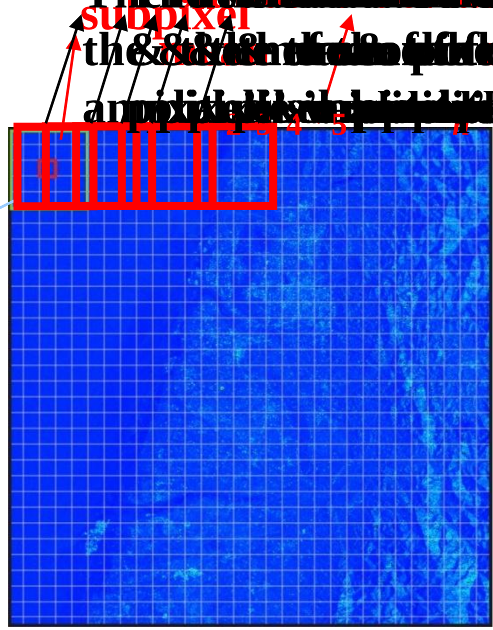

Amplitude Data

σ_A and μ_A are the standard deviation and the mean of a series of amplitude values, respectively.

$$\mu_A = \frac{1}{n}\sum_{i=1}^{n} V_{A(i)}$$

$$\sigma_A = \sqrt{\frac{1}{n}\sum_{i=1}^{n}\left(V_{P(i)} - \overline{V_{P(i)}}\right)^2}$$

The amplitude dispersion index, , is defined by Ferretti et al. [2001] as

$$D_A \equiv \frac{\sigma_A}{\mu_A} \qquad (1)$$

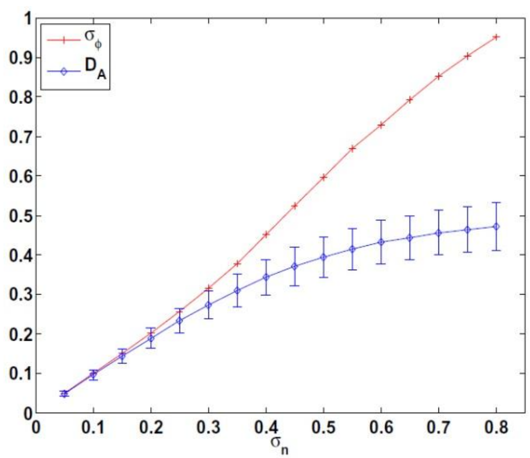

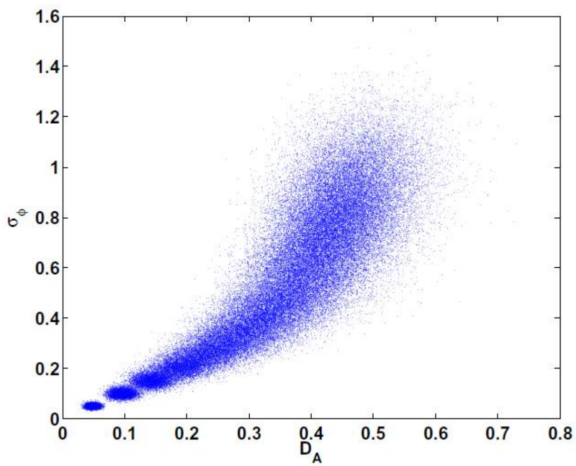

There is a statistical relationship between amplitude stability and phase stability, consideration of amplitude is useful both to reduce the number of pixels for phase analysis, and to better estimate the probability of a pixel being a PS.

[Ferretti et al., 2001; Hooper et al., 2007]

$$\phi_{x,i} = \phi_{def,x,i} + \phi_{\alpha,x,i} + \phi_{orb,x,i} + \phi_{\varepsilon,x,i} + n_{x,i} \quad (2)$$

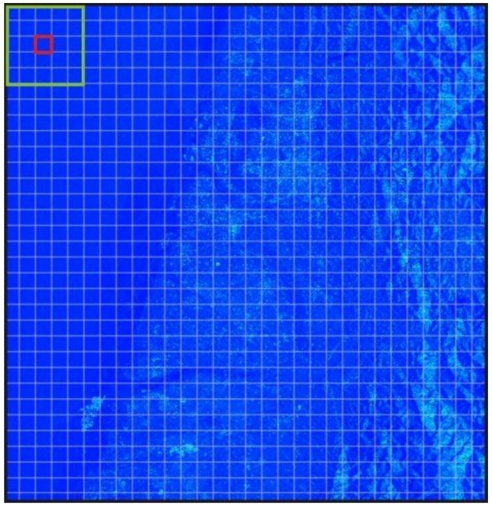

Phase Data

ϕ_{def} is the phase change due to movement of the pixel in the satellite line-of-sight direction

ϕ_{ε} is the residual phase due to look angle error (DEM error)

ϕ_{α} is the phase due to the difference in atmospheric delay between passes

ϕ_{orb} is the residual phase due to satellite orbit inaccuracies

n is a noise term due to variability in scattering, thermal noise, co-registration errors etc.

We define a measure of the variation of this residual phase for a pixel as

$$\gamma_x = \frac{1}{N}\left|\sum_{i=1}^{N} \exp\{\sqrt{-1}\left(\phi_{x,i} - \tilde{\phi}_{x,i} - \Delta\hat{\phi}^{u}_{\varepsilon,x,i}\right)\}\right|$$

where N is the number of interferograms

$\tilde{\phi}_{x,i}$ is a wrapped estimate of the spatially correlated parts of each of the terms

$\Delta\hat{\phi}^{u}_{\varepsilon,x,i}$ denotes the spatially uncorrected part of $\phi_{\varepsilon,x,i}$

ASAR images from Track 232, Frame 3123 of ENVISAT

In this paper, we used 20 images from August 2006 to September 2008 to estimate vertical displacements over CRAF

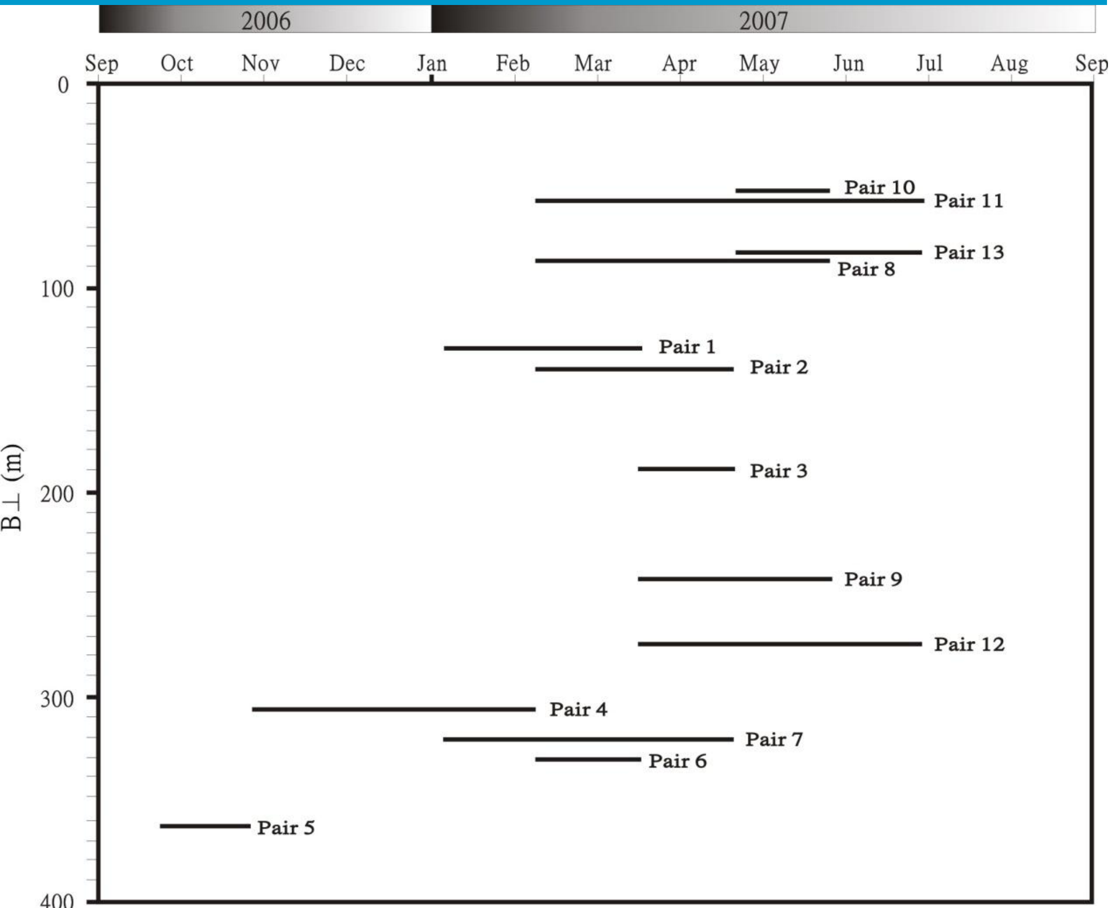

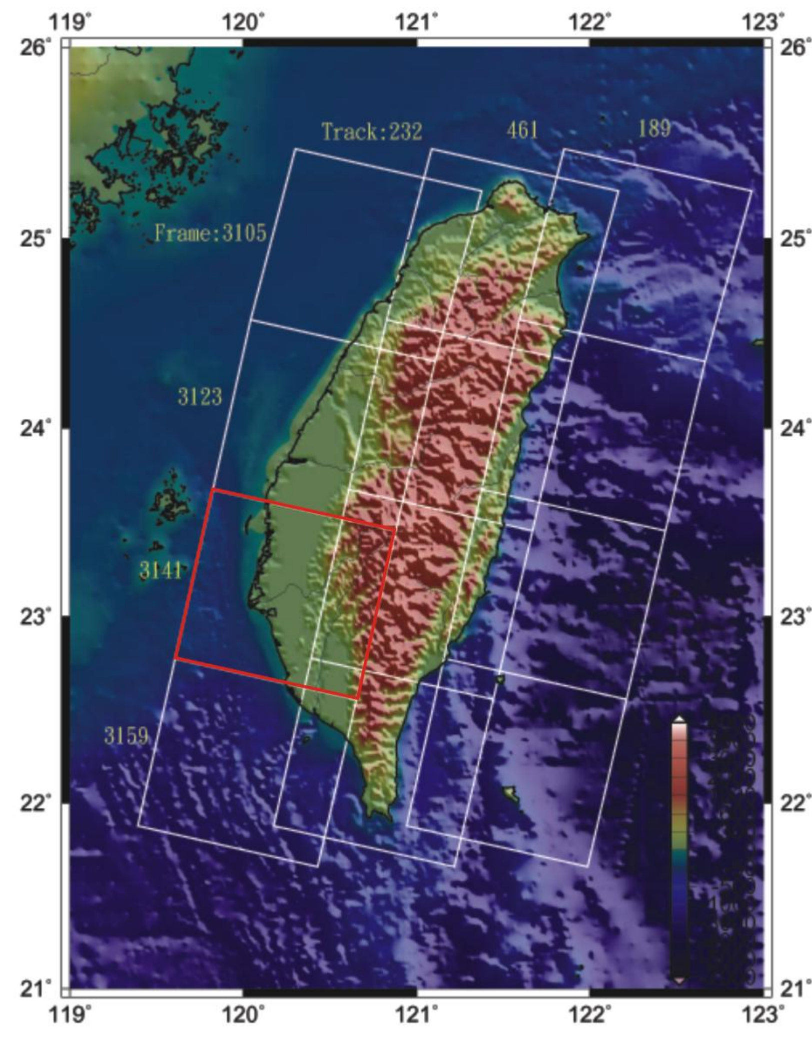

PSI Result

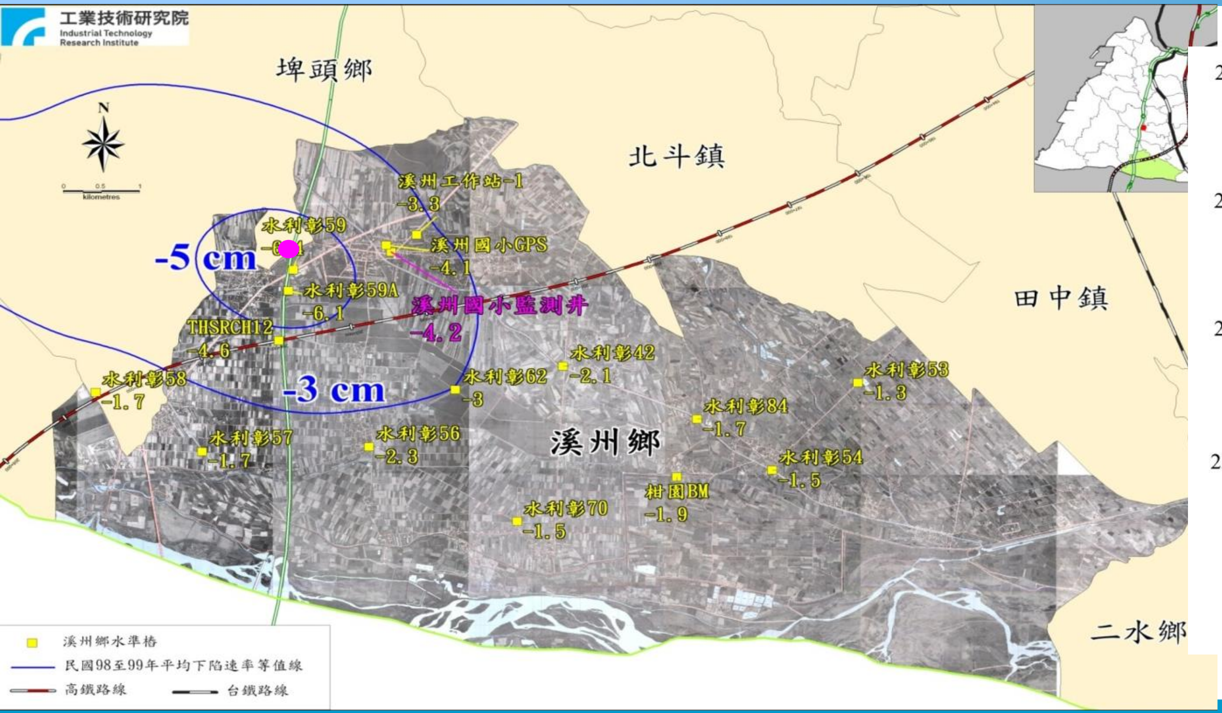

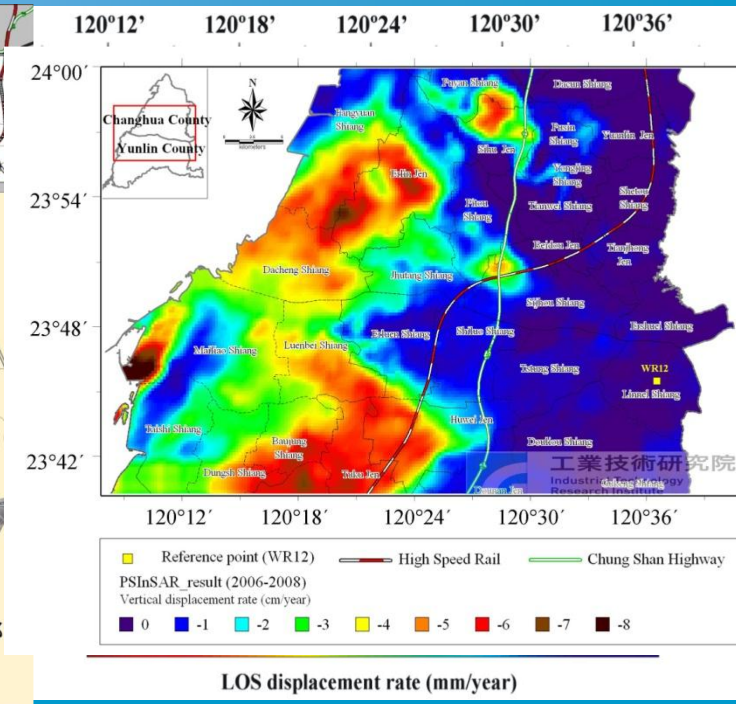

The 20 time-series interferograms over the 2006-2008 period

The 20 interferograms were stacked to obtain the mean LOS displacement rates

Vertical Displacement from PSI Result

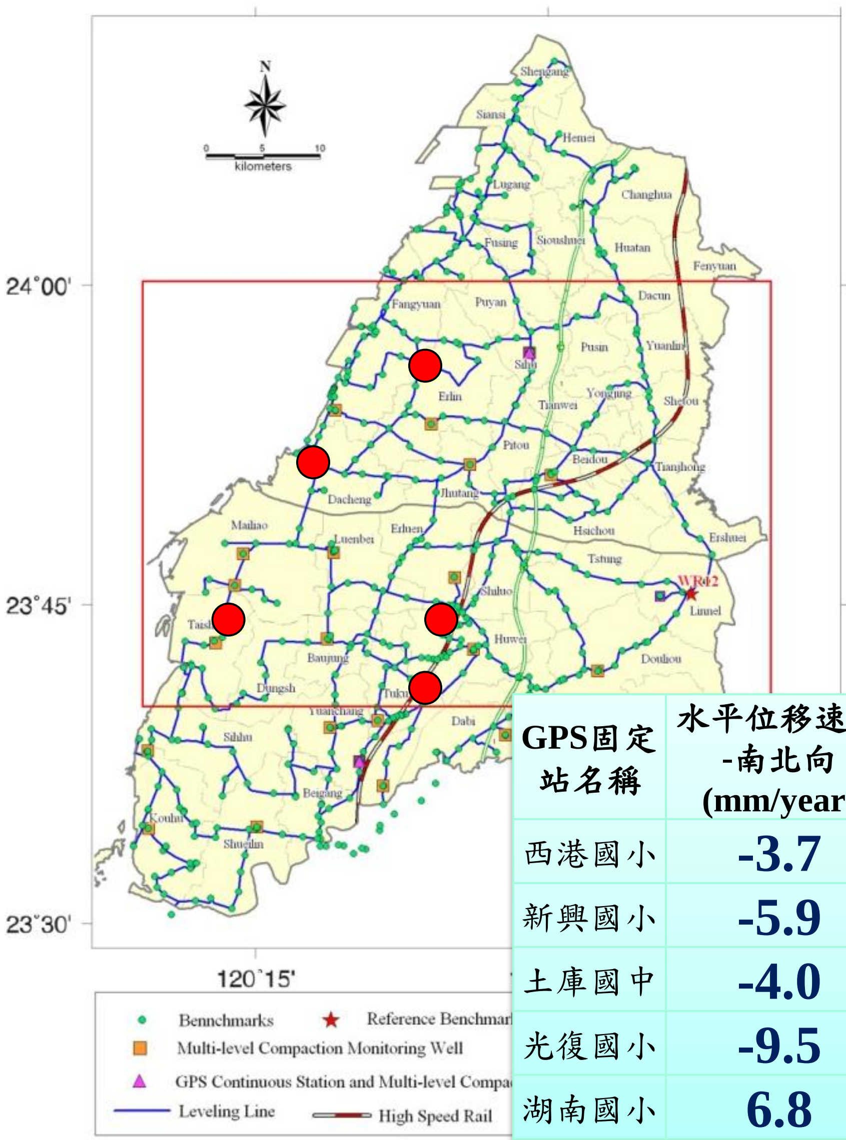

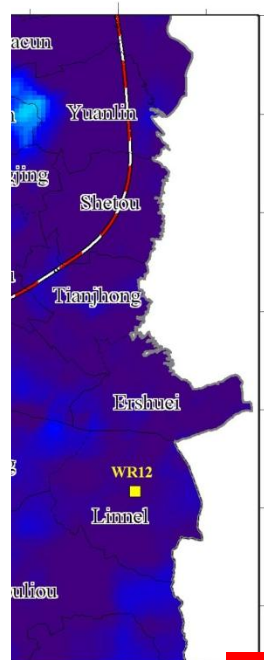

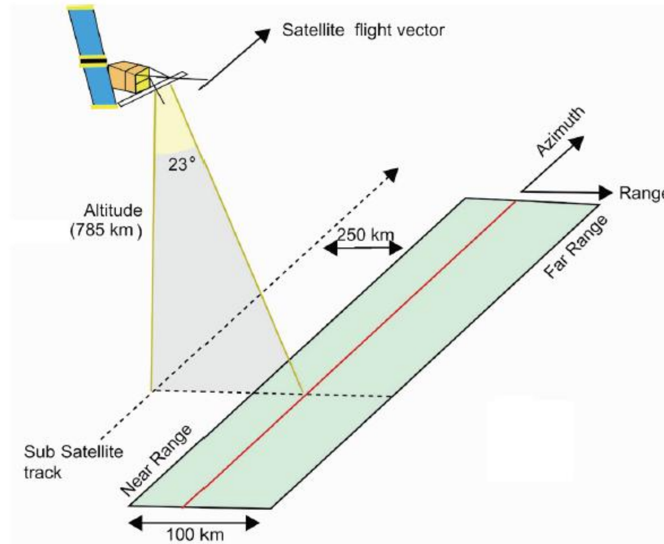

$$\delta r = (a\cos\varphi + b\sin\varphi)\sin\theta + c\cos\theta$$

where δr: LOS Displacement

GPS固定站名稱	水平位移速率-南北向 (mm/year)	水平位移速率-東西向 (mm/year)	水平位移速率投影至LOS方向位移速率 (mm/year)	PSI LOS方向位移速率 (mm/year)	水平向位移影響PSI觀測值之比率（%）
西港國小	-3.7	2.6	1.3	-43.4	2.9
新興國小	-5.9	2.0	1.2	-23.1	5.2
土庫國中	-4.0	4.3	1.9	-54.3	3.5
光復國小	-9.5	1.2	1.3	-46.0	2.8
湖南國小	6.8	2.5	0.3	-34.0	0.9

Cross Validation

294 Benchmarks in 1523km^2 0.19 points/km^2

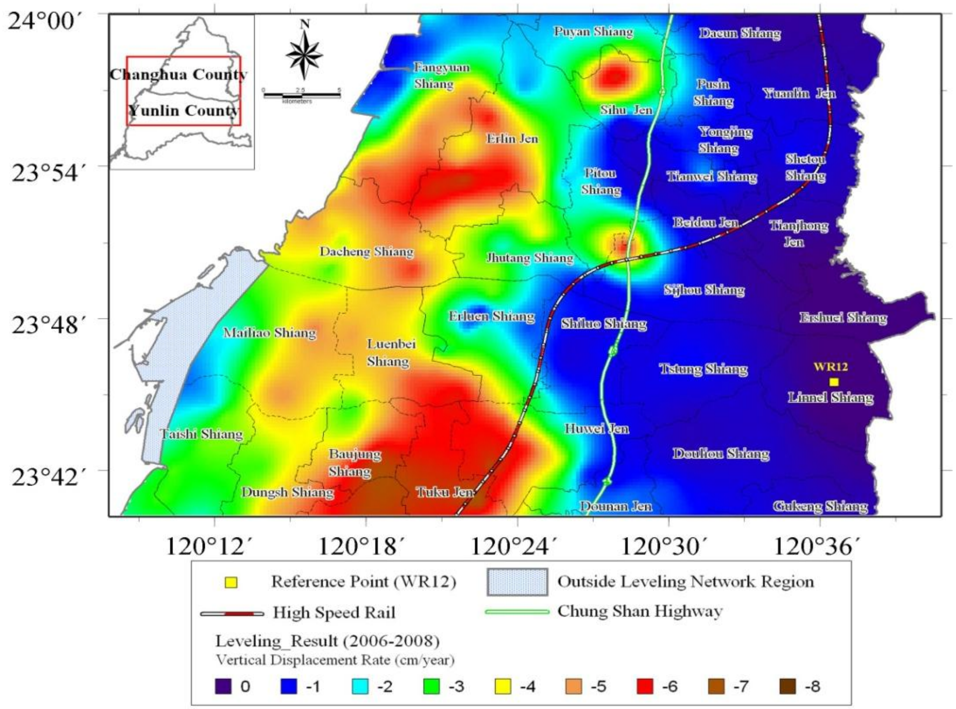

153413 PS pixels in 1523km^2: 107.6 pixels/km^2

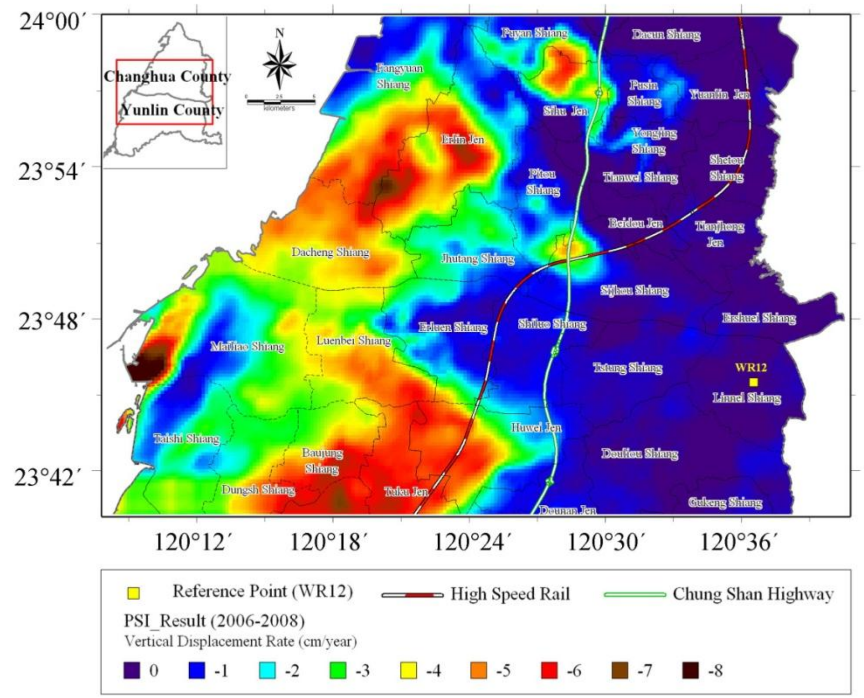

(Hung et al., 2011)

1. Density 2. Boundary 3. Industrial Park

Comparison of vertical displacements between PSI and Leveling

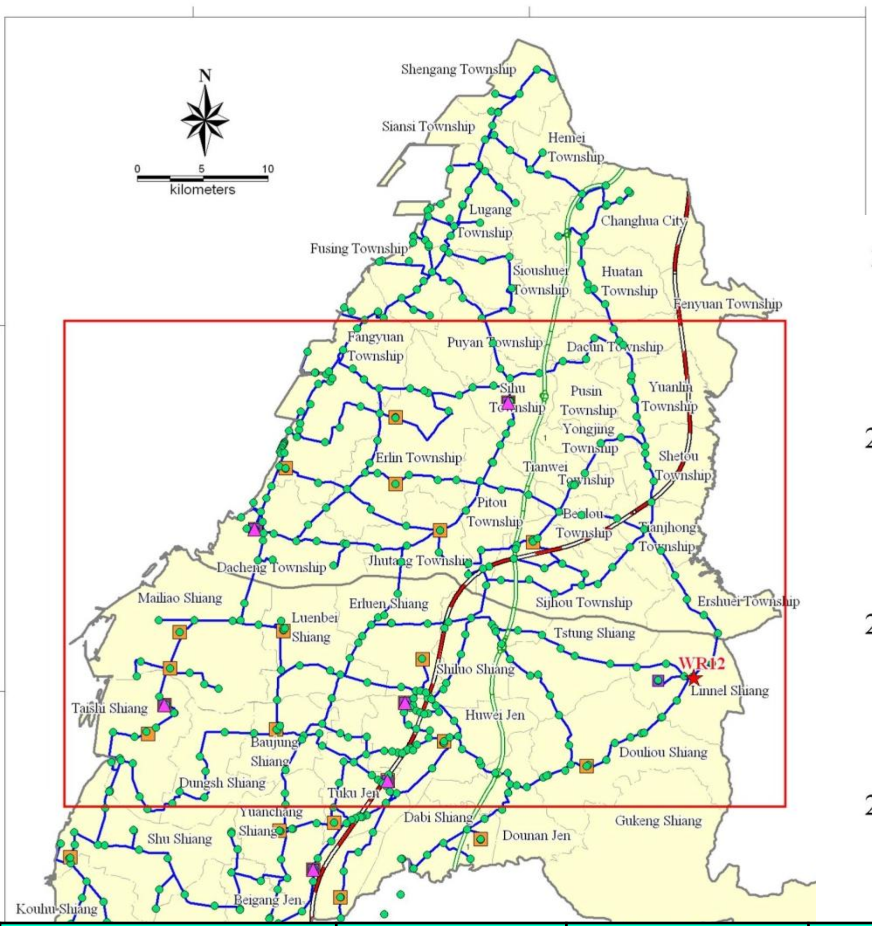

88%（257）差異量在 ±1 公分以內

12%（37） 差異量在 ±1～2 公分以內

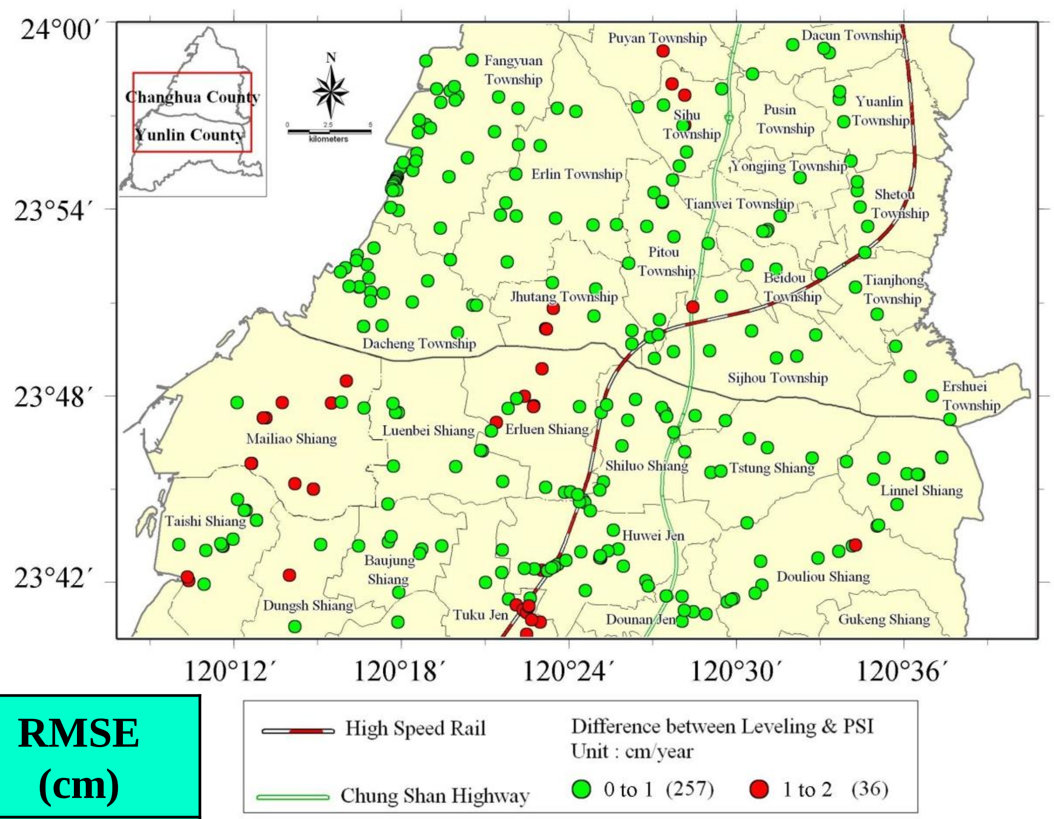

Comparison between Leveling and PSI	Within ± 1cm	Within ± 1～2 cm	RMSE (cm)
	257	36	0.6

Summary of causes of large difference

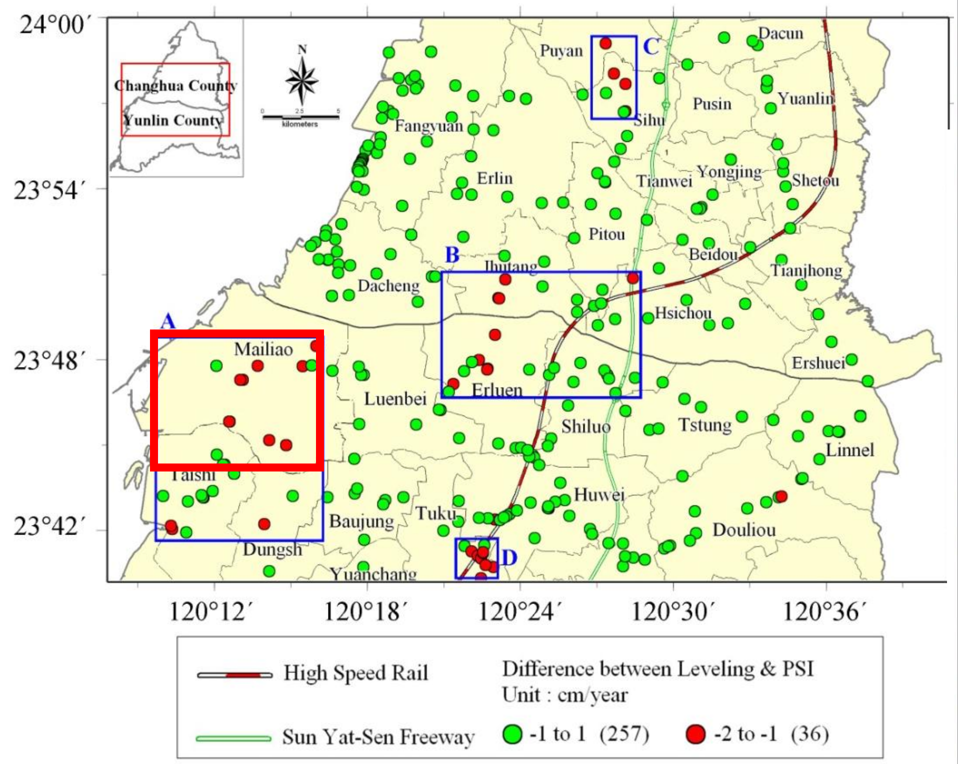

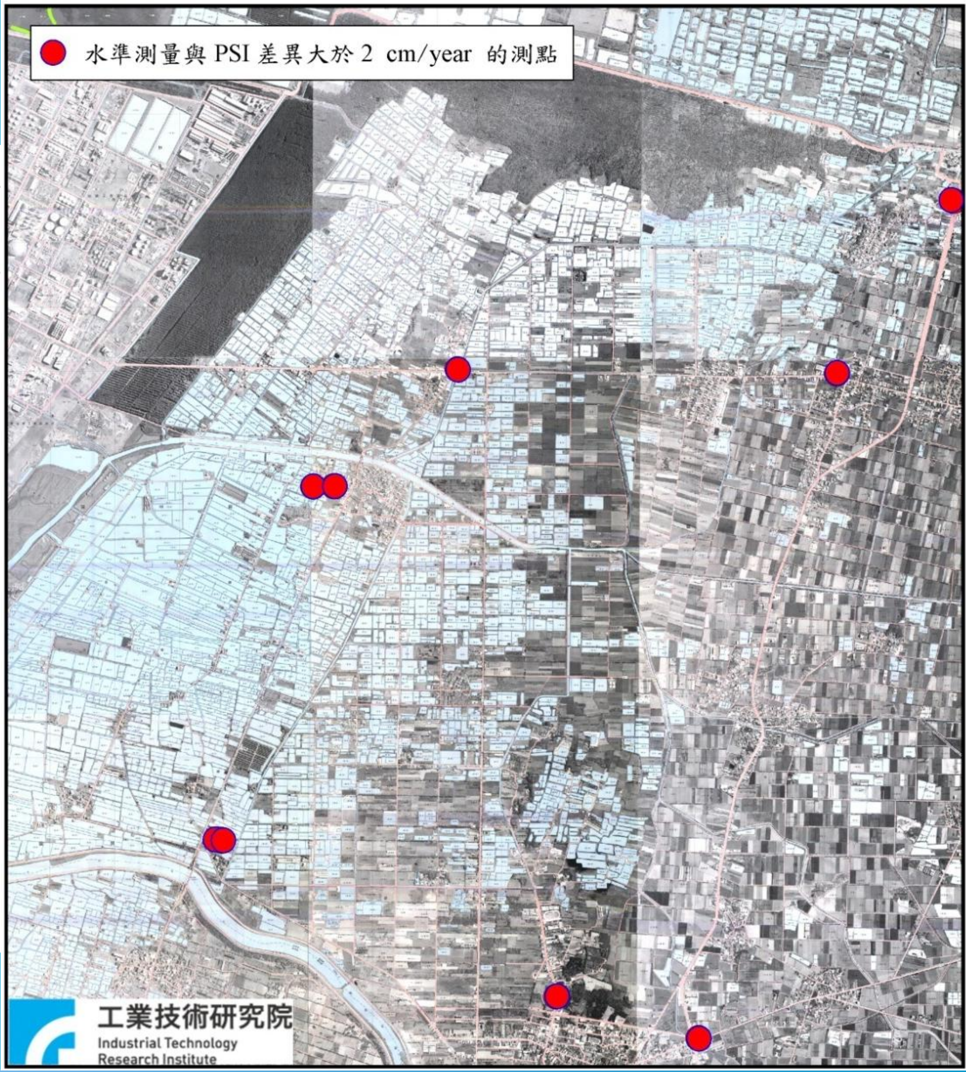

Fusion of PSI and leveling-derived vertical displacements

- Leveling ： High Vertical Accuracy; Low Density
- PSI ： Low Vertical Accuracy; High Density

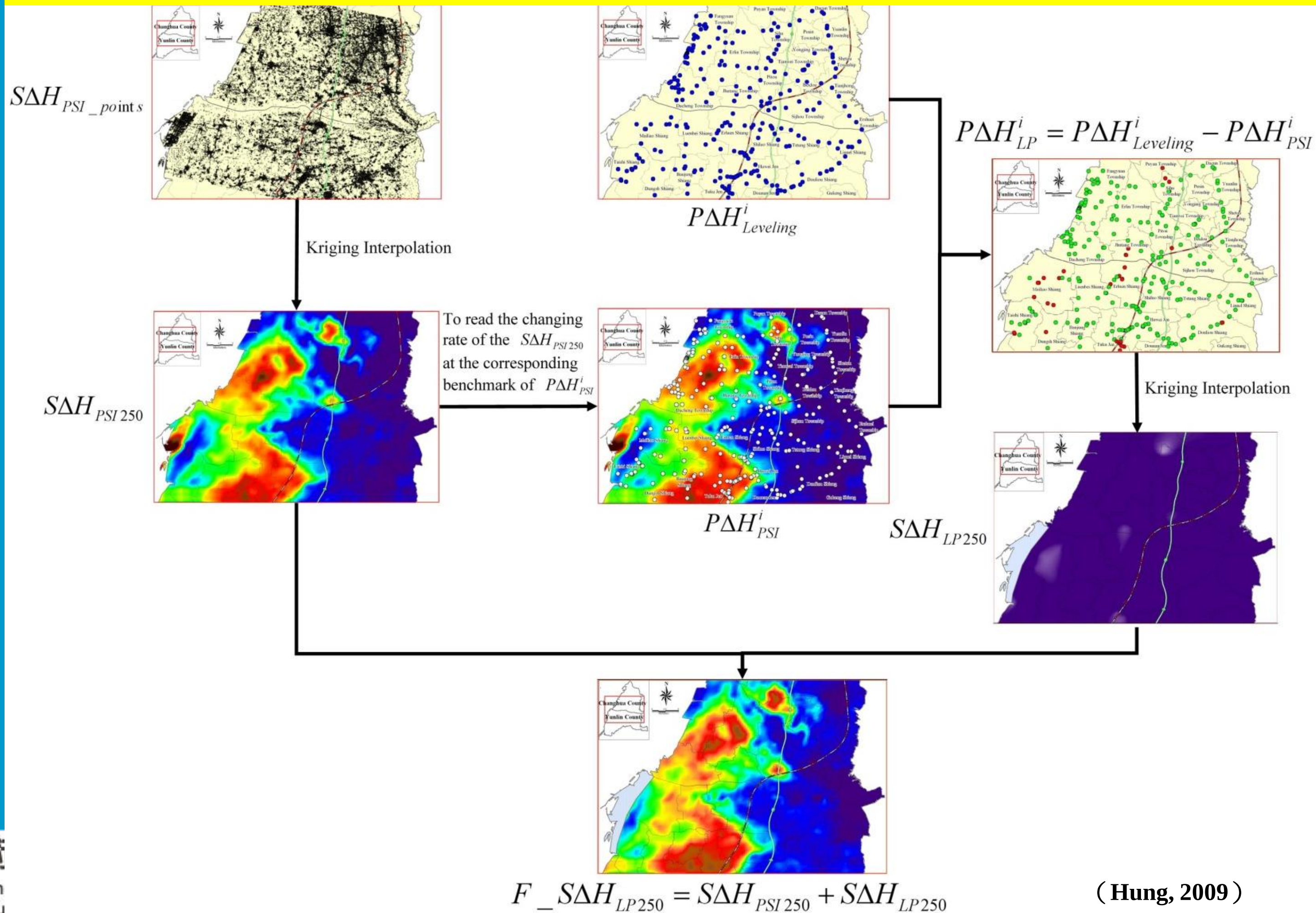

（Hung, 2009）

Comparison of vertical displacements between PSI and Leveling

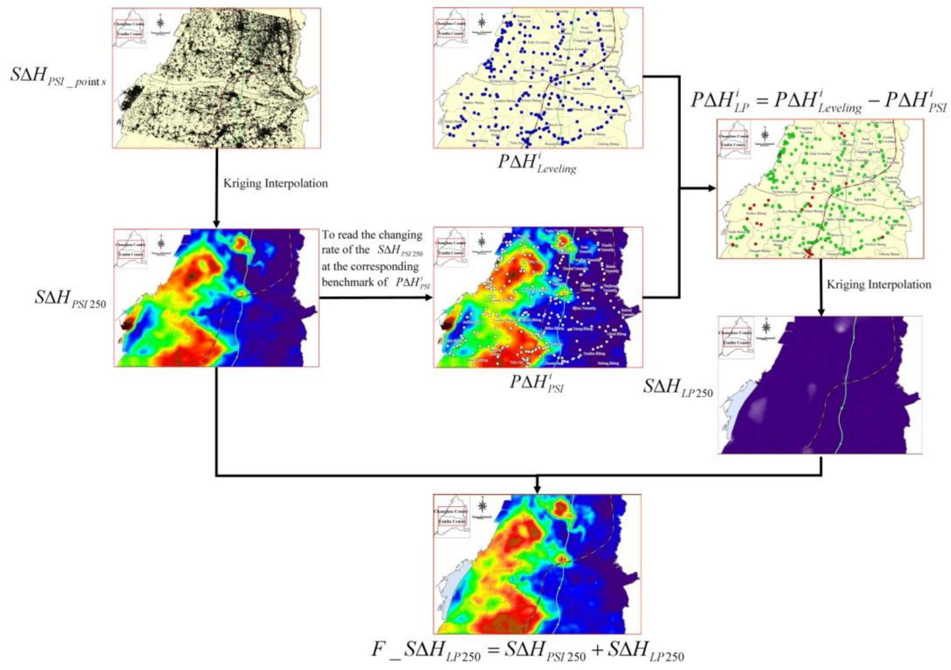

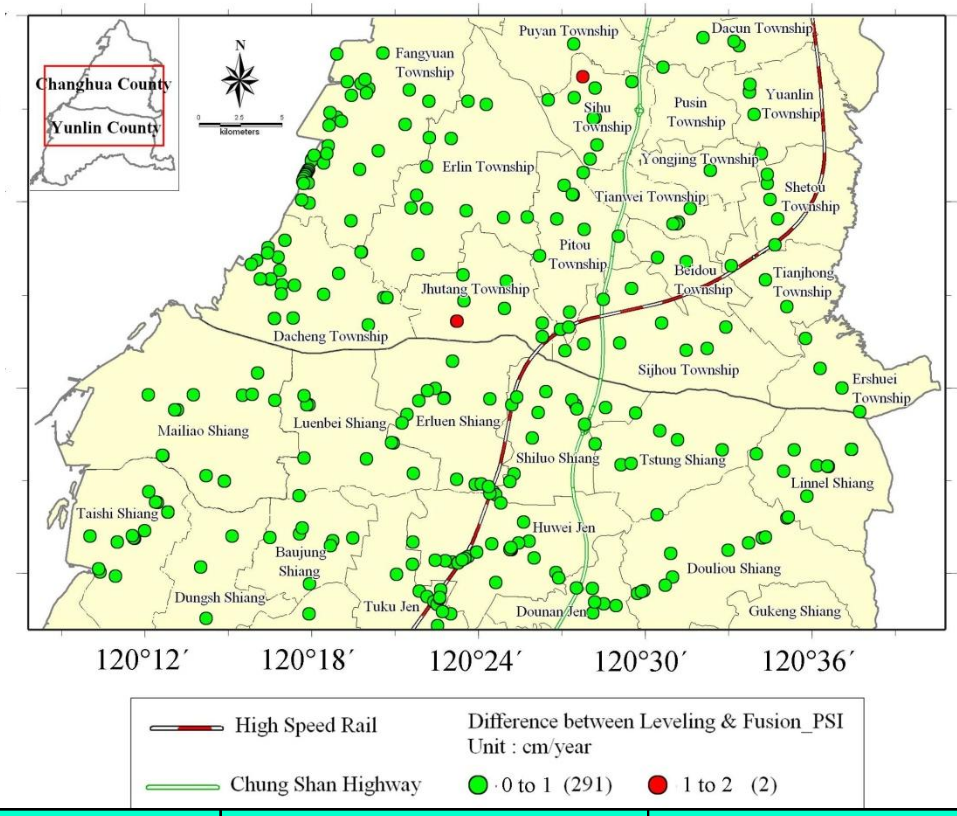

The difference between Leveling and PSI		Within ± 1cm	Within ± 1～2 cm	RMSE (cm)
Benchmark（point）	Original Result	257 (88%)	36 (12%)	0.6
	Combined Result	291 (99%)	2 (1%)	0.4

5. Discussion and Conclusions

- **PSI Benefit**
  - More detailed spatial and temporal coverage
  - Better represents the overall subsidence pattern.
- **Future Work**
  - Wavelet functions or Spectral combinations can be employed.
  - Use PSI to monitor Taiwan's deformation, validated by 300 continuous GPS stations